ADVANCING EARTH AND SPACE SCIENCE

JGR Solid Earth

RESEARCH ARTICLE

10.1029/2021JB021684

Key Points:

- In the United States, 96 of 161 volcanoes have at least one type of detected activity (seismicity, deformation, and gas or thermal emissions)
- Forty-five percent of volcanoes with thermal emissions are only seen by medium-spatial resolution satellites (<100 m/pixel)
- Each volcano has an Activity Intensity Level; a higher score from multiple data types indicates a greater likelihood of magmatic activity

Supporting Information:

Supporting Information may be found in the online version of this article.

Correspondence to:

M. E. Pritchard,
pritchard@cornell.edu

Citation:

Reath, K., Pritchard, M. E., Roman, D. C., Lopez, T., Carn, S., Fischer, T. P., et al. (2021). Quantifying eruptive and background seismicity, deformation, degassing, and thermal emissions at volcanoes in the United States during 1978–2020. *Journal of Geophysical Research: Solid Earth*, *126*, e2021JB021684. https://doi.org/10.1029/2021JB021684

Received 15 JAN 2021
Accepted 13 MAY 2021

Quantifying Eruptive and Background Seismicity, Deformation, Degassing, and Thermal Emissions at Volcanoes in the United States During 1978–2020

K. Reath[1], M. E. Pritchard[1], D. C. Roman[2], T. Lopez[3], S. Carn[4], T. P. Fischer[5], Z. Lu[6], M. P. Poland[7], R. G. Vaughan[8], R. Wessels[9], L. L. Wike[1,10], and H. K. Tran[1]

[1]Earth and Atmospheric Sciences, Cornell University, Ithaca, NY, USA, [2]Earth and Planets Laboratory, Carnegie Institution for Science, Washington, DC, USA, [3]Geophysical Institute, University of Alaska Fairbanks, Fairbanks, AK, USA, [4]Geological and Mining Engineering and Sciences, Michigan Technological, Houghton, MI, USA, [5]Department of Earth and Planetary Sciences, University of New Mexico, Albuquerque, NM, USA, [6]Department of Earth Sciences, Southern Methodist University, Dallas, TX, USA, [7]U.S. Geological Survey—Cascades Volcano Observatory, Vancouver, WA, USA, [8]U.S. Geological Survey—Astrogeology Science Center, Flagstaff, AZ, USA, [9]U.S. Geological Survey Headquarters, Reston, VA, USA, [10]Now at Department of Geology, University of Maryland, College Park, MD, USA

Abstract An important aspect of volcanic hazard assessment is determination of the level and character of background activity at a volcano so that deviations from background (called unrest) can be identified. Here, we compile the instrumentally recorded eruptive and noneruptive activity for 161 US volcanoes between 1978 and 2020. We combine monitoring data from four techniques: seismicity, ground deformation, degassing, and thermal emissions. To previous work, we add the first comprehensive survey of US volcanoes using medium-spatial resolution satellite thermal observations, newly available field surveys of degassing, and new compilations of seismic and deformation data. We report previously undocumented thermal activity at 30 volcanoes using data from the spaceborne ASTER sensor during 2000–2020. To facilitate comparison of activity levels for all US volcanoes, we assign a numerical classification of the Activity Intensity Level for each monitoring technique, with the highest ranking corresponding to an eruption. There are 96 US volcanoes (59%) with at least one type of detected activity, but this represents a lower bound: For example, there are 12 volcanoes where degassing has been observed but has not yet been quantified. We identify dozens of volcanoes where volcanic activity is only measured by satellite (45% of all thermal observations), and other volcanoes where only ground-based sensors have detected activity (e.g., all seismic and 62% of measured degassing observations). Our compilation provides a baseline against which future measurements can be compared, demonstrates the need for both ground-based and remote observations, and serves as a guide for prioritizing future monitoring efforts.

Plain Language Summary We have compiled the instrumentally recorded eruptive and noneruptive activity in terms of earthquakes, ground deformation, degassing, and thermal emissions for 161 US volcanoes between 1978 and 2020. There are 96 US volcanoes (59%) with at least one type of detected activity. But we think that more than 96 volcanoes had activity during this time period because of the limits in the data available. We report previously undocumented thermal activity at 30 volcanoes using data from the spaceborne ASTER sensor measured in the Thermal Infrared during 2000–2020. We identify dozens of volcanoes where volcanic activity is only measured by satellite (45% of all thermal observations), and other volcanoes where only ground-based sensors have detected activity (e.g., all seismic and 62% of measured degassing observations). Our compilation provides a baseline against which future measurements can be compared, demonstrates the need for both ground-based and remote observations, and serves as a guide for prioritizing future monitoring efforts.

1. Introduction

Unlike most geohazards, volcanic eruptions are often preceded by warning signs, including increased seismicity, ground deformation, degassing, or thermal emissions from hours to months (or even years) before eruption (e.g., UNESCO, 1971). Such preeruptive unrest is defined as "the deviation from the background or baseline behavior of a volcano towards a behavior which is a cause for concern in the short-term because it might prelude an eruption" (Phillipson et al., 2013). Implicit in this definition of unrest is a quantification of

10.1029/2021JB021684

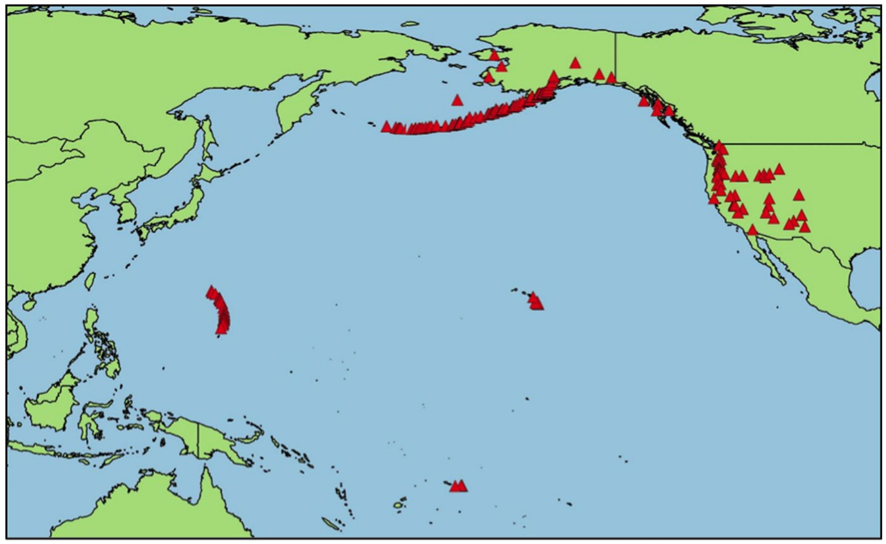

Figure 1. The locations of the 161 volcanoes included in this study (red triangles), all within the territory of the United States.

the background level of volcanic activity such that increases can be discerned. However, many volcanoes in the United States (US) have inadequate background observations for one or more monitoring data types—that is, seismicity, ground deformation, and gas or thermal emissions (Ewert, 2007; Ewert et al., 2005). Even where background volcanic activity has been measured at US volcanoes, there is no existing compilation that can be queried with fundamental questions such as How many US volcanoes have had detectable activity? Are these detections made on the ground, by satellites, or both? Are certain erupting or nonerupting volcanoes more (or less) likely to show activity with multiple types of monitoring data (seismicity, deformation, and gas or thermal emissions)?

Here, we combine new analyses of ground and satellite monitoring observations with information from the scientific literature to create a compilation of multiparameter observations of volcanic activity at 161 US volcanoes (Figure 1) between 1978 and 2020. We define volcanic activity as seismicity, thermal output, gas emission, and ground deformation of likely magmatic or hydrothermal origin as defined in the peer-reviewed literature. We also make note of deformation and seismic activity that have been measured at a volcano but are not related to magmatic or hydrothermal activity, such as tectonic earthquakes or near-surface processes like lava flow subsidence, faulting, and geothermal power production (see Section 2.3). Our focus is on activity that has been instrumentally recorded by ground-, airborne, and satellite-based instruments, instead of inferred to have happened in the absence of measurements, as done in some previous studies (e.g., Ewert et al., 2018).

In our compilation, we characterize both background volcanic activity and volcanic unrest (i.e., deviations from background) in order to identify the highest level of activity whether associated with eruption or not. Volcanic unrest in the US was considered by Diefenbach et al. (2009) and updated by Ewert et al. (2018); this paper adds to those compilations by identifying any volcanoes with measured activity even if that activity is not considered unrest. For many volcanoes, the level of activity changes with time, but those changes are not considered here. By only recording the highest level of activity, we can highlight two critical measurements: (a) for volcanoes that did not erupt, the highest amount of noneruptive volcanic activity present over ~40 years (between 1978 and 2020, including both unrest and background activity) and (b) for volcanoes that did erupt, the amount of instrumentally detected activity during eruption.

We characterize activity for 161 volcanoes in our compilation, taken from the U.S. Geological Survey (USGS) assessment of volcanoes that pose a threat (Ewert et al., 2018). While there are 169 US volcanoes of Holocene age (i.e., eruptions in the last ~12,000 years) listed in the Volcanoes of the World (VOTW) compilation (Global Volcanism Program, 2013), the eight volcanoes that are in the VOTW but not in our compilation are deep submarine or otherwise considered to have a very low threat even if they have eruptions since

1978 (e.g., Lōʻihi, Hawaiʻi, NW Rota 1, Vailuluʻu, and Mariana Back-Arc Segment at 15.5°N). The list of potentially active volcanoes changes with time as new information is collected and so should be revisited periodically—see Ewert et al. (2018) for detailed rationale of volcanoes added and removed relative to Ewert et al. (2005). We focus on volcanoes with Holocene activity as "potentially active," along with some Pleistocene US volcanoes that were included in the USGS threat assessment (Yellowstone, Long Valley, and Coso; Ewert, 2007; Ewert et al., 2005, 2018). Future work should better document mud volcanoes which erupt and pose hazards that can be monitored by satellite (e.g., Niu et al., 2019) and areas of potential magmatic unrest where there is no obvious associated vent such as Strandline Lake, AK (Kilgore et al., 2011) and Socorro, NM (e.g., Fialko & Simons, 2001), as well as several seismic swarms in the western Great Basin (e.g., Hatch-Ibarra, 2020; Smith et al., 2004, 2016).

We use ground-based, airborne, and space-based observations of gas and thermal emissions and ground deformation, and ground-based observations of seismic activity. We build on previous work by including additional data sets, such as the first comprehensive survey of US volcanoes from 2000 to 2020 using medium-spatial resolution satellite thermal observations (90 m/pixel) from the ASTER (Advanced Spaceborne Thermal Emission and Reflection Radiometer) instrument, newly available field surveys of gas emissions, and new compilations of seismic and deformation data. Over time, data quality and quantity have increased for all monitoring types that we consider (e.g., Carn et al., 2016; Hooper et al., 2018; Power et al., 2019; Wright et al., 2004); however, a major source of uncertainty in our compilation is that the quality of available data varies with space, time, and data type. We have chosen to include measurements from 1978 to 2020 because the first satellite observations of volcanic activity in the form of elevated emissions of sulfur dioxide (SO_2) begin in 1978 (e.g., Carn et al., 2016), even though for most US volcanoes monitoring data are not available from all techniques starting at that time. For example, satellite observations of ground deformation from Interferometric Synthetic Aperture Radar (InSAR) began in the 1990s, and the quality of those data has varied over time (e.g., Dzurisin et al., 2019; Lu & Dzurisin, 2014). Satellite thermal data were not used quantitatively until the 1980s, even though low-resolution data have been available from weather satellites since the 1960s (Harris, 2013). In Section 2, we further describe the different types of monitoring data that we include in our study.

We present our compilation of multiparameter observations of volcanic activity at 161 US volcanoes from 1978 to 2020 as two supplementary files: one for volcanoes with eruptive activity (Table S1) and the other for volcanoes that did not have instrumentally recorded eruptions during that interval (Table S2). Future work could have separate Activity Intensity Level (AIL) during eruptive and noneruptive periods for each volcano, but in this study, there is a single, maximum AIL per volcano. For each volcano, we record whether activity has been detected from each of the four monitoring methods along with a reference to the source of information. Further, we include a numerical classification of the intensity of activity and whether the activity was detected by ground, airborne, or spaceborne sensors. Higher ranks indicate a higher level of activity, which, if seen in multiple data sets, may indicate a higher likelihood of magmatic activity. While the idea of using a single ranking across monitoring data types is inspired by the Volcano Unrest Index (Potter et al., 2015), we use a simpler ranking scheme that can be applied to a large number of volcanoes with heterogeneous data. We then use the compiled data to (a) develop an integrated ground- and satellite-based assessment of eruptive and noneruptive volcanic activity in the US (including intensity and type of activity) and (b) compare the activity among volcanoes in the US as measured by space- and ground-based sensors and different monitoring techniques to identify areas that may require additional attention when considered in a larger context of risk-mitigation or scientific objectives.

2. Methods

In the following subsections, we document the seismic, gas and thermal emissions, and ground deformation data that were used to characterize volcanic activity at the 161 volcanoes. For each type of monitoring data, an AIL from 0 to 3 has been defined and applied, with the highest value (AIL = 3) corresponding to detections made during eruption and AIL = 0 indicating no detections related to new magmatic activity (Table 1). For ground deformation, there may be detected activity that has an AIL = 0 if any ground deformation is caused by cooling of older lava flows, faulting, or human activities (i.e., pumping/injection at geothermal power plants)—see Section 2.3. For all monitoring types, at rank 0, there may still be low-level

Table 1
The Types of Observed Activity That are Considered When Ranked Using the AIL

AIL value	Thermal	Degassing	Deformation	Seismic
3	Eruptive detection by low-spatial resolution satellites (MODIS; ~1 km/pixel)	Eruptive detection by satellite monitoring	Directly related to eruptive magmatic processes	Eruptive seismic signals
2	Noneruptive detection by manual analysis of medium-spatial resolution (90 m/pixel) ASTER data	Noneruptive detection by satellite monitoring	Directly related to noneruptive magmatic processes	Noneruptive swarms (or other diagnostic seismic signals) with magmatic origins
1	Noneruptive detection through ground-based or airborne sources	Noneruptive detection and measurement by ground-based or airborne instruments	Ambiguous origins may be magmatic or nonmagmatic	Swarms with unclear origins or background earthquakes of whatever type (VT, LF, VLP, LP, etc.)
0.5		Noneruptive identification by ground-based visual observations		
0	No detection or clearly not of current magmatic origin			

Note. A more detailed explanation of the criteria used in the rankings can be found in Sections 2.1–2.4.
Abbreviation: AIL, Activity Intensity Level.

volcanic activity present, but not detected either because there are no local/satellite observations or the detection threshold of the available data sets is not low enough.

It is difficult to compare low levels of volcanic activity (AIL 1 and 2) from the different types of monitoring data (e.g., Potter et al., 2015), so slightly different criteria are used for each monitoring type. For gas and thermal emissions, we assume that only more vigorous activity can be measured from space, so volcanic activity detected by satellite has AIL = 2 and activity only detected by ground or airborne sensors has AIL = 1. A rank of 0.5 is included for gas emissions that have been seen but not measured (see Section 2.2). It would be better to use the gas flux or measured temperatures in the AIL, but given the heterogeneity in types of data available (e.g., satellite pixel size, location where ground measurements are made, etc.) this is not yet possible. For the seismic and deformation techniques, AIL = 1 indicates activity with an ambiguous origin and AIL = 2 indicates a presumed magmatic source. Although it is difficult to separate magmatic and nonmagmatic activity (e.g., Pritchard et al., 2019), we cite previous interpretations of the origin of seismic and deformation activity. We acknowledge that the assessment of AIL is subjective and that different investigators might come up with different assessments; nevertheless, this assessment serves as a good starting point for understanding volcanoes whose magmatic systems may be more active than previously documented—indeed, ambiguity and disagreement between experts highlights the need for a better understanding of causative processes.

The objective of creating the AIL is to quickly and easily identify volcanoes with high scores of activity seen in multiple data sets. For each volcano, we sum the AIL from the four monitoring techniques. The maximum summed AIL ranking is 12 and the maximum for a volcano without detected eruptions is 8. Our hypothesis is that volcanoes with high AIL in multiple categories are more likely to erupt and merit close scrutiny. An important caveat for the AIL ranking is that not all volcanoes are well monitored during the entire period—for example, some volcanoes could have magmatic seismicity but only ranked as AIL = 0 because there is no seismic network to make the needed measurements.

2.1. Thermal Activity

Thermal activity was identified using satellite observations via automated detection algorithms and manual observation, as well as airborne and ground-based observations. An AIL = 3 for thermal denotes detections of thermal features that occurred during an eruption and were made through automated detection algorithms, specifically Moderate Resolution Imaging Spectroradiometer Volcano (MODVOLC; Wright, 2016; Wright et al., 2004) and Middle InfraRed Observation of Volcanic Activity (MIROVA; Coppola et al., 2016).

10.1029/2021JB021684

These algorithms are based on Moderate Resolution Imaging Spectroradiometer (MODIS) data, which have a ~1-km pixel size in the Thermal Infrared (TIR) wavelengths and span 2000–2020. For a thermal feature to be detected with this pixel size, it must either cover a relatively large area or have a high temperature (Poland et al., 2020).

AIL 2 classifications of thermal activity are noneruptive and are not large or hot enough to be routinely detected by MODIS or any currently available automated detection algorithms. They can, however, be detected by the ASTER sensor, which has a higher-spatial resolution than MODIS—90 m/pixel in the TIR. Reath, Pritchard, Moruzzi, et al. (2019) found that the most sensitive automated detection algorithm based on MODIS data, MIROVA, was incapable of detecting thermal features with temperature <20°C above background in the 90 m/pixel ASTER images, while the sensitivity of ASTER is ~2°C. The only automated detection algorithm for these data, the ASTER Volcano Archive, is not optimized for low-temperature thermal features (Pieri et al., 2007). Therefore, we performed a manual analysis of the ASTER TIR nighttime imagery following the methods outlined by Reath, Pritchard, Moruzzi, et al. (2019) and Reath, Pritchard, Poland, et al. (2019) using the ASTER Product 8 temperature derived using the method of Gillespie et al. (1998). We focused on nighttime imagery because it is easier to detect low amplitude thermal anomalies at night. Other satellite data with spatial resolution <100 m/pixel in the TIR, like Landsat 8, do not routinely collect nighttime images and cannot currently be used for quantitative analysis (Reath, Pritchard, Moruzzi, et al., 2019).

Any noneruptive observation of thermal activity made from airborne or ground-based instrumentation that has not been detected by satellite has been classified as Rank 1. These detections primarily consist of airborne surveys made with a thermal camera but also include measurements made from a radiometer, a ground-based thermal camera, or any other nonsatellite heat-detection devices (e.g., Friedman et al., 1982; Hill & Prejean, 2005; Moxham, 1970).

2.2. Degassing Activity

We consider any volcanic gas species (e.g., H_2O, CO_2, SO_2, and H_2S) whether detected through ground-based, airborne, or satellite remote sensing, or quantified by direct sampling of gas emitted from fumaroles, steaming ground, or bubbling springs to be indicative of degassing-related activity. In most cases, particularly with satellite detections, these observations are limited to SO_2 due to the relative ease of detecting this gas in the ultraviolet (UV) and TIR wavelengths. Many of these detections have been made by the TOMS and OMI sensors in the UV and the MODIS and IASI sensors in the TIR (e.g., Carn et al., 2016, 2017; Fioletov et al., 2016). However, the detection limit for these sensors is high due to large pixel sizes (e.g., 13 × 24 km for OMI) combined with the lack of automated detected algorithms for TIR data (e.g., Carn et al., 2008). At volcanoes where SO_2 is detected and quantified by satellite during an eruption, AIL = 3. When satellite observations are made of noneruptive volcanic degassing, AIL = 2. While it is not always easy to distinguish eruptive from noneruptive degassing from space, for simplicity we use the catalog of Carn et al. (2016) to describe eruptive degassing and that of Carn et al. (2017) to describe noneruptive degassing.

For AIL = 1, we include degassing measurements made from ground-based methods as well as airborne sensors (e.g., Doukas & McGee, 2007; Symonds, Poreda, et al., 2003; Werner et al., 2011). Airborne measurements have the advantage of lower detection thresholds compared to satellites, whereas ground-based observations have an increased level of sensitivity, can quantify a broader range of gas species, and certain techniques are capable of collecting near continuous data at the volcanoes with permanently installed sensors (e.g., Lopez et al., 2017). Airborne and ground-based techniques also allow gases to be measured in situ, enabling volcanic gases such as CO_2 and H_2O to be quantified, even though those species are present in large quantities in background air and therefore extremely difficult to detect from space (e.g., Poland et al., 2020). Additionally, many ground-based detections are made through direct sampling using Giggenbach flasks, which are capable of making highly sensitive discriminations of volcanic gas compositions (e.g., Giggenbach, 1975, 1996) at the time of the sampling but cannot measure flux. All of these factors increase the sensitivity of measuring volcanic degassing from the ground and airborne sensors beyond what can be detected by satellite monitoring. The disadvantage of the ground and airborne measurements of degassing is that not all volcanoes are monitored equally and/or consistently given limits on accessibility. For this reason, not all degassing volcanoes in the US have been measured with ground or airborne instrumentation.

Many volcanoes emit plumes of steam or condensed water vapor (and potentially other gases) that can be seen visually but that have not been quantified. The presence of vapor plumes implies a subsurface heat source and in many cases corresponds with mixtures of hydrothermal and volcanic gases (e.g., Fischer et al., 2019). However, we do not consider observations of steam or bubbling hot springs to be indicative of volcanic degassing without compositional data to confirm or refute a magmatic source. Therefore without compositional data, we cannot assign visible observations of degassing AIL values with the same level of confidence as the previously mentioned ranks. Nevertheless, as there is a chance these volcanoes with only visual observations and no measurements are indicative of magmatic degassing, we have assigned them a degassing rank of 0.5.

2.3. Deformation Activity

Ground deformation at volcanoes is measured from space (InSAR) and by terrestrial sensors (Global Positioning System, tilt, Electronic Distance Measurements, etc.) (e.g., Dzurisin, 2006). The AIL values for recorded deformation activity are based on how the deformation correlates to eruptive and potential magmatic subsurface processes. Unlike with the thermal and degassing classifications, we have made no distinction between measurements made by satellite or the ground instruments because both can produce measurements of similar accuracy, although they have different capabilities in terms of spatial and temporal resolution (e.g., Dzurisin, 2006). Deformation on or around volcanoes, however, is not always clearly attributable to subsurface magmatic activity (e.g., Hill & Prejean, 2005; Intrieri et al., 2013; Lu & Dzurisin, 2014). Deformation observed during an eruption has AIL = 3. Deformation that can be directly related to magmatic processes but not eruption (e.g., Amelung et al., 2007; Lu, 2007; Poland et al., 2017) is given an AIL = 2. Volcanoes having deformation with ambiguous origins have AIL = 1—in these cases, it is unclear if the deformation is primarily related to magmatic, faulting/seismic, or other processes (e.g., Crowell et al., 2013; Lu, 2007; Poland, 2010). We have identified deformation that is known to be related to surficial processes, such as the cooling of lava or pyroclastic flows, flank creep, faulting, and anthropogenic activity like geothermal power production (e.g., Dietterich et al., 2012; Dzurisin et al., 2002; Ebmeier et al., 2012; Howle et al., 2003; Intrieri et al., 2013; Wittmann et al., 2017) in a separate column (Tables 2 and 3, Tables S1 and S2). We include these types of deformation so that the surficial or anthropogenic activity is not confused in the future with deformation related to magmatic processes but do not assign an elevated ranking based on this deformation (i.e., AIL = 0).

2.4. Seismic Activity

Similar to deformation, the AIL in seismic activity is ranked based on whether seismic activity is thought to be related to eruptive, magmatic, or ambiguous activity. Sensitivity to seismicity is a function of the nature of seismic instrumentation surrounding a volcano. A comprehensive map and list of the locations of the permanent (and some campaign) volcano-seismic monitoring networks in the US can be found at ds.iris.edu/gmap (network codes AV, CC, HV, MI, NC, NN, UU, and UW) and in Alaska by Power et al. (2019). We record the current seismic monitoring level as a column in Tables S1 and S2 based on the criteria of Moran et al. (2008).

An AIL ranking of 3 for seismic activity is assigned when seismicity can be directly linked with an eruptive event (e.g., Neal et al., 2019; Power et al., 2004; Roman & Cashman, 2018). AIL = 2 seismicity relates to swarms that are likely related to magma intrusion (e.g., Farrell et al., 2010; Roman & Power, 2011; Syracuse et al., 2015). There are additional potential seismic indicators of magma intrusion (e.g., deep LPs, some kinds of tremor, drum beats, mixed phase "hybrid" events) but we do not use these as catalogs do not routinely record them. Finally, seismic swarms or earthquakes that have an unclear cause (i.e., that may be due to magmatic activity or to tectonic/hydrothermal activity) (e.g., Dixon et al., 2015; Murphy et al., 2014) are assigned an AIL = 1. Additionally, systems with nonnegligible seismic activity (e.g., a nonzero background event rate or occasional LF events; e.g., Gareloi) are assigned an AIL = 1. For volcanoes with AIL = 0, no elevated seismicity has been observed, either because of a lack of earthquake activity or because the monitoring was poor.

Table 2
Activity Observed by Ground and Satellite Sensors for All US Volcanoes (N = 31) With Eruptive Activity Between 1978 and 2020

Name	Submarine (Y/N)[32]	Year of eruption(s) (1978–2020)[32,a]	US volcano threat ranking[1]	Thermal activity (0–3)	Degassing activity (0–3)	Deformation activity (0–3)	Surficial or other deformation (Y/N)	Seismic activity (0–3)	AIL sum
Kīlauea	N	2020, 1983–2018, 2020	1	3 [3,4]	3 [10,11,99]	3 [19]	Y[136]	3 [29]	12
Mount St. Helens	N	2004–2008, 1990–1991, 1989–1990, 1980–1986	2	3 [3,4]	3 [12,100,101]	3 [18]	Y[18]	3 [30]	12
Redoubt	N	2009, 1989	4	3 [3,4]	3 [10,12,102,103]	3 [53,b]	Y[17]	3 [30,121,122]	12
Augustine	N	2005–2006, 1986	12	3 [3,4]	3 [10–12,104,105]	3 [16,17]	Y[17]	3 [30]	12
Mauna Loa	N	1984	16	3 [4,88,93]	3 [12,88,116]	3 [20,88,b]	Y[28]	3 [48, 88]	12
Okmok	N	2008, 1997, 1986–1988, 1983, 1981	19	3 [4,7,9b]	3 [12,64,84]	3 [16,17]	Y[17]	3 [30]	12
Veniaminof	N	2018, 2013, 2008, 2002–2006, 1995, 1993–1994, 1987, 1983–1984	29	3 [3,4]	3 [10,11]	3 [17]	N	3 [123,124]	12
Anatahan	N	2007–2008, 2006, 2004–2005, 2003	63	3 [3,4]	3 [10–12,106,107]	3 [25,c]	N	3 [43]	12
Korovin	N	2006, 2005, 2004, 2002, 1998, 1987	31	2 [4]	3 [10,64]	3 [17]	N	3 [108,125,d]	11
Shishaldin	N	2019–2020, 2014–2015, 2004, 1999, 1998, 1997, 1995–1996, 1993, 1986–1987, 1979, 1978	32	3 [3,4]	3 [10–12,109]	1 [74]	N	3 [35]	10
Pagan	N	2012, 2011, 2010, 2006, 1996, 1993, 1992, 1988, 1987, 1981–1985	44	3 [3,4]	3 [10,12,40]	3 [23,135]	Y[65]	1 [40]	10
Cleveland	N	2020, 2016–2019, 2005–2015, 2001, 1997, 1994, 1987, 1986, 1984	48	3 [3,4,7]	3 [10,110,111]	1 [138]	Y[17]	3 [90]	10
Semisopochnoi	N	2018–2020, 1987	55	1 [4]	3 [117]	3 [42]	Y[17]	3 [42]	10
Spurr	N	1992	10	2 [4,95]	3 [10–12,15,112]	1 [17]	N	3 [35]	9
Pavlof	N	2016, 2014, 2013, 2007, 1996–1997, 1990, 1986–1988, 1983, 1981, 1980	41	3 [3,4,7]	3 [12,59]	0	N	3 [35]	9
Bogoslof	N	2016–2017, 1992	76	3 [4,9b]	3 [75]	0 [13]	N	3 [44]	9
Makushin	N	1995, 1993–1994, 1987, 1980	9	2 [4]	2 [55,64,73]	2 [16,17]	N	2 [34,87]	8
Kasatochi	N	2008	47	2 [4,96]	3 [12]	0	N	3 [32]	8
Fourpeaked[e]	N	2006	53	0	2 [12,15,41]	3 [17]	N	3 [41]	8
Akutan	N	1992, 1991, 1990, 1989	8	2 [4,98]	1 [54,55,73,76–78]	2 [16,17]	N	2 [34]	7
Westdahl	N	1991–1992	36	2 [4,97]	0	3 [16,17]	N	1 [51]	6
Kanaga	N	2012, 1995, 1994	39	2 [4,97]	1 [61]	0 [17]	Y[17]	3 [51]	6
Great Sitkin	N	2019, 2018	46	2 [4]	1 [64]	0	N	3 [35]	6
South Sarigan Seamount	Y	2010	119	0	3 [32,118]	0	N	3 [32]	6
Kiska	N	1990	70	2 [4]	1 [32]	2 [16,17]	N	0	5
Seguam	N	1993, 1992	50	2 [4,97]	0	2 [16,17]	Y[17]	0	4
Gareloi	N	1989, 1987, 1982, 1980	60	2 [4]	2 [10,11,73]	0 [17]	Y[17]	1 [89]	4
Chiginagak	N	1998	71	2 [4,92]	2 [10,11]	0	N	0	4

Table 2
Continued

Name	Submarine (Y/N)[32]	Year of eruption(s) (1978–2020)[32,a]	US volcano threat ranking[1]	Thermal activity (0–3)	Degassing activity (0–3)	Deformation activity (0–3)	Surficial or other deformation (Y/N)	Seismic activity (0–3)	AIL sum
Ahyi seamount	Y	2014, 2001	158	1 [67]	0	0	N	3 [32]	4
Amukta	N	1997, 1996, 1987	91	2 [4,97]	0	1 [17]	Y[17]	0	3
Ruby	Y	1995	159	0	0	0	N	3 [46]	3

Notes. Dates of eruptions and whether the volcano is submarine are from VOTW. Volcanoes are ordered by AIL values (explained in Section 2)—those with the same AIL are then ranked by their threat ranking from Ewert et al. (2018). Additional information for each volcano including comparison with Ewert et al. (2018) is available in Table S1. Superscripts refer to important references for each monitoring type at each volcano which is not meant to be complete (because some volcanoes have dozens of studies): [1]Ewert et al. (2018). [2]Poland et al. (2019). [3]Wright (2016). [4]ASTER analysis performed for this study. [5]Moxham (1970). [6]Friedman et al. (1982). [7]Although a thermal feature was reported at a Katmai Lake by Dehn et al. (2000), subsequent analysis revealed it to be an artifact of solar reflection by Dehn et al. (2011). [8]Bergfeld et al. (2006). [9]Hill and Prejean (2005). [9b]Coppola et al. (2016). [10]Carn et al. (2017). [11]Fioletov et al. (2016). [12]Carn et al. (2016). [13]Topographic change measured by satellite but not deformation: Waythomas et al. (2020). [14]Werner et al. (2008). [15]Doukas and McGee (2007). [16]Lu (2007). [17]Lu and Dzurisin (2014). [18]Poland et al. (2017). [19]Poland et al. (2015). [20]Amelung et al. (2007). [21]Dzurisin et al. (2019). [22]Marshall et al. (1997). [23]Banks et al. (1984). [24]Crowell et al. (2013). [25]Trusdell et al. (2005). [26]Tizzani et al. (2007). [27]Fialko and Simons (2000). [28]Poland (2010). [29]Neal et al. (2019). [30]Roman and Cashman (2018). [31]Thelen (2016). [32]Global Volcanism Program (2013). [33]Dzurisin et al. (2006). [34]Syracuse et al. (2015). [35]Power et al. (2004). [36]Prejean et al. (2002). [37]Murphy et al. (2014). [38]Roman and Power (2011). [39]Farrell et al. (2010). [40]Lyons et al. (2016). [41]Gardine et al. (2011). [42]DeGrandpre et al. (2019). [43]Pozgay et al. (2005). [44]Wech et al. (2018). [45]Brumbaugh et al. (2014). [46]Koyanagi et al. (1993). [47]Wicks et al. (2001). [48]Okubo and Wolfe (2008). [49]Miller et al. (1998). [50]McGimsey et al. (2014). [51]Cameron et al. (2017). [52]Dixon et al. (2015). [53]Grapenthin et al. (2013). [54]Lu et al. (2000). [55]Symonds, Janik, et al. (2003). [56]Craig et al. (1978). [57]Moran et al. (2008). [58]Kwoun et al. (2006). [59]Collected during field campaign by Lopez et al. (2017). [60]Lopez et al. (2017). [61]Fischer and Lopez (2016). [62]Werner, Kern, et al. (2020). [63]Mitchell et al. (2010). [64]Howle et al. (2003). [65]Henderson et al. (2019). [66]Crider et al. (2011). [67]Embley et al. (2007). [68]Baker et al. (2008). [69]Hill (1984). [70]Fierstein and Hildreth (2008). [71]https://volcanoes.usgs.gov/volcanoes/coso_volcanic_field/. [72]Carn et al. (2003). [73]Fischer et al. (2019). [74]Gong et al. (2015). [75]Lopez et al. (2020). [76]Bergfeld et al. (2013). [77]Motyka et al. (1993). [78]Symonds, Poreda, et al. (2003). [79]Evans et al. (2015). [80]Cameron et al. (2020). [81]Cameron and Snedigar (2016). [82]Werner et al. (2009). [83]Werner et al. (2011). [84]Bergfeld et al. (2020). [85]Evans et al. (2009). [86]Wech et al. (2020). [87]Lanza et al. (2020). [88]Lockwood et al. (1985). [89]Caplan-Auerbach and Prejean (2005). [90]Power et al. (2017). [91]Reath et al. (2010). [92]Schaefer et al. (2008). [93]Patrick and Witzke (2011). [94]Vaughan et al. (2012). [95]Schneider and Rose (1995). [96]Waythomas et al. (2010). [97]Dehn et al. (2011). [98]Kienholz et al. (2009). [99]Elias et al. (2020). [100]Casadevall et al. (1983). [101]Gerlach et al. (2008). [102]Werner et al. (2013). [103]Lopez et al. (2013). [104]Symonds et al. (1992). [105]McGee et al. (2010). [106]De Moor et al. (2005). [107]McCormick et al. (2015). [108]Neal et al. (2009). [109]Kearney (2005). [110]Werner et al. (2017). [111]Werner, Rasmussen, et al. (2020). [112]Doukas and Gerlach (1995). [114]Dixon et al. (2008). [115]Lopez et al. (2019). [116]Greenland (1987). [117]TROPOMI analysis. [118]AIRS, OMI, and GOME-2 analysis. [119]Hildreth et al. (2001). [120]West et al. (2005). [121]Chouet et al. (1994). [122]Power et al. (2013). [123]Cameron et al. (2018). [124]Pesicek et al. (2018). [125]Jiang and Lohman (2020). [126]Lynch et al. (2013). [127]Mazzini et al. (2011). [128]Trugman et al. (2016). [129]Christenson et al. (2007). [130]Goff and Janik (2002). [131]Sherrod et al. (1997). [132]Wagner et al. (2018). [133]Nathenson and Mariner (2013). [134]Embley et al. (2004). [135]Sako et al. (1995). [136]Dietterich et al. (2012). [137]Dzurisin et al. (2002). [138]Wang et al. (2015). [139]McLaughlin and Donnelly-Nolan (1981). [140]Evans et al. (2004). [141]Crankshaw et al. (2018). [142]Ingebritsen and Mariner (2010). [143]Moussa and Kiser (2018).

[a]Twenty-kilometer SSE of Hayes, deformation was seen along with seismic activity at Strandline Lake that is thought to be of magmatic origin (reference 17). [b]Eruptive (AIL = 3) deformation only detected by ground-based sensors, not InSAR. [c]Deformation is only detected by ground-based sensors. [d]Eruptions at Chiginagak in 1998 and Korovin in 2002, 2004, 2005, and 2006–2007 are confirmed in the VOTW eruption catalog but are either questionable or do not exist in the AVO catalog. [e]The 2006 eruption at Fourpeaked is classified as a phreatic eruption, but that it was likely triggered by the intrusion of new magma.[41]

2.5. Eruptive Activity

We use the database of eruptions and dates of eruption for US volcanoes from the VOTW (Global Volcanism Program, 2013), as it provides a uniform reference for all US eruptions. We include notes where eruptions listed as confirmed in the VOTW (for example at Korovin and Chiginagak) are not listed or are listed as questionable in the Alaska Volcano Observatory eruption catalog (Alaska Volcano Observatory, 2021). One phreatic eruption is included at Fourpeaked volcano where a shallow magmatic intrusion is inferred to have occurred (Gardine et al., 2011).

3. Results

Our compilation of volcanic activity detections is provided as two separate tables, for volcanoes with eruptions in the VOTW (Table S1; abridged version in Table 2) and those without recorded eruptions (Table S2; abridged version in Table 3). Of the 161 volcanoes considered here, 31 had instrumentally recorded eruptions during the study period; however, not all monitoring techniques have measurements during all eruptions.

Table 3
Activity Observed by Ground and Satellite Sensors for the Subset (N = 68) of US Volcanoes With AIL > 0 (or Surficial or Nearby Deformation: Hualālai, Hayes, and Yunaska) but No Eruptive Activity

Name	Submarine (Y/N)[32]	US volcano threat ranking[1]	Thermal activity (0–3)	Degassing activity (0–3)	Deformation activity (0–3)	Surficial or other deformation (Y/N)	Seismic activity (0–3)	Sum AIL
Baker	N	14	2 [4]	1 [32,55,73,78,82]	2 [18,a]	N	2 [66]	7
Yellowstone	N	21	2 [4,94]	1 [14,56]	2 [21]	N	2 [39]	7
Martin	N	25	2 [4]	1 [15,60,73]	2 [17]	N	2 [50]	7
Lassen Volcanic Center	N	11	2 [4,5]	1 [56,73]	2 [18]	N	1 [32]	6
Long Valley	N	18	1 [8,73]	1 [8]	2 [21,22,26]	Y[64]	2 [36]	6
Iliamna	N	20	2 [4]	1 [15,83,73]	1 [17]	N	2 [38]	6
Aniakchak	N	22	2 [4]	1 [58,73]	2 [16,17]	N	1 [35]	6
Mageik	N	26	2 [4]	1 [15,55,60,73,78]	2 [17]	N	1 [37]	6
Trident	N	27	2 [4]	1 [55,60,73,78]	2 [17]	N	1 [37]	6
Douglas	N	54	2 [4]	1 [15,73]	2 [17]	N	1 [52]	6
Takawangha	N	84	2 [4]	0	2 [17]	N	2 [32]	6
Three Sisters	N	7	1 [140]	0	2 [18]	N	2 [33]	5
Atka	N	30	2 [4]	1 [64,73,77]	2 [17]	N	0	5
Medicine Lake	N	45	1 [141]	1 [141]	2 [18]	Y[137]	1 [33]	5
Salton Buttes	N	56	2 [4,91]	1 [126,127]	1 [24,125]	Y[125]	1 [128]	5
Tanaga	N	61	0	1 [115]	2 [17]	N	2 [50]	5
Mammoth Mountain	N	90	1 [9,73]	1 [9]	1 [9]	N	2 [36]	5
Rainier	N	3	2 [4,5]	1 [55,78]	0	N	1 [31]	4
Hood	N	6	2 [4,6]	1 [55,78]	0	N	1 [33]	4
Ugashik-Peulik	N	40	0	1 [85]	2 [16,17]	N	1 [52]	4
Fisher	N	51	2 [4]	1 [62]	1 [17]	N	0	4
Coso Volcanic Field	N	72	1 [71]	1 [71,129]	1 [27,47]	Y[27,47]	1 [71,128]	4
Little Sitkin	N	75	2 [4]	1 [49,79]	0	N	1 [51]	4
Kupreanof	N	93	2 [4]	0.5 [80,81]	2 [17]	N	0	4
Wrangell	N	101	2 [4]	1 [64]	0	N	1 [120]	4
Shasta	N	5	1 [5]	1 [55,78]	0	N	1 [32]	3
Newberry	N	13	1 [141]	1 [131,132]	0	N	1 [31]	3
Novarupta	N	37	2 [4]	0.5 [80,81]	1 [17]	Y[17]	0 [37]	3
Emmons Lake	N	73	0	1 [64,79]	2 [17]	N	0	3
Mono-Inyo Craters	N	24	0	0.5 [69]	2 [22,26]	N	0 [36]	2.5
Herbert	N	113	2 [4]	0.5 [80,81]	0	N	0	2.5
Clear Lake	N	33	1 [139]	0	0	N	1 [32]	2
Alamagan	N	62	2 [4]	0	0	N	0 [32]	2
Recheschnoi	N	67	0	1 [64,84]	1 [17]	N	0	2
Mono Lake Volcanic Field	N	69	0	0	2 [26]	N	0 [36]	2
Adagdak	N	79	0	1 [64]	0	N	1 [35]	2
San Francisco Volcanic Field	N	80	0	0	0	N	2 [45]	2
Black Peak	N	89	2 [4]	0	0	N	0	2
Ukinrek Maars	N	92	0	1 [85]	0	N	1 [32]	2
Farallon de Pajaros	N	95	2 [4]	0	0	N	0	2
Mauna Kea	N	106	0	0	0	N	2 [86]	2

Table 3
Continued

Name	Submarine (Y/N)[32]	US volcano threat ranking[1]	Thermal activity (0–3)	Degassing activity (0–3)	Deformation activity (0–3)	Surficial or other deformation (Y/N)	Seismic activity (0–3)	Sum AIL
Tana	N	108	0	1 [62,79]	0	N	1 [90]	2
Supply Reef	Y	118	0	0	0	N	2 [32]	2
Wide Bay	N	128	0	0	0	N	2 [87]	2
Kukak	N	66	0	0.5 [80,81]	0	N	1 [1]	1.5
East Diamante	Y	97	1 [67]	0.5 [67]	0	N	0	1.5
Kasuga 2	Y	156	1 [68]	0.5 [68]	0	N	0	1.5
Diakoku seamount	Y	157	1 [67]	0.5 [67]	0	N	0	1.5
Glacier Peak	N	15	1 [141]	0	0	N	0	1
Crater Lake	N	17	1 [142]	0	0	N	0	1
Katmai	N	28	0 [7]	0	0	N	1 [37]	1
Adams	N	34	0	1 [134]	0	N	0	1
Griggs	N	42	0	1 [55,78]	0	N	0 [37]	1
Agrigan	N	57	0	1 [63,73]	0	N	0	1
Dutton	N	64	0	0	0	N	1 [49]	1
Valles Caldera	N	68	0	1 [130]	0	N	0	1
Sarigan	N	96	0	0	0	N	1 [32]	1
Asuncion Island	N	103	1 [32]	0	0	N	0	1
Maug Islands	N	122	1 [67]	0	0	N	0	1
Indian Heaven	N	131	0	0	0	N	1 [143]	1
Esmeralda Bank	Y	160	1 [67]	0	0	N	0	1
Kaguyak	N	43	0	0.5 [70]	0	N	0	0.5
Snowy Mountain	N	52	0	0.5 [119]	0	N	0	0.5
Kagamil	N	100	0	0.5 [80,81]	0	N	0	0.5
Zealandia Bank	N	109	0	0.5 [134]	0	N	0	0.5
Hualālai	N	23	0	0	0 [28]	Y[28]	0	0
Hayes	N	35	0	0	0 [b]	N	0	0
Yunaska	N	98	0	0	0[17]	Y[17]	0	0

Notes. The full list ($N = 130$) including additional information for each volcano is available in Table S2. Volcanoes are ordered by summed AIL values (explained in Section 2)—those with the same AIL are then ranked by their threat ranking from Ewert et al. (2018). Superscripts refer to references (see note to Table 2).
Abbreviation: AIL, Activity Intensity Level.
[a]Deformation is only detected by ground-based sensors. [b]20 km SSE of Hayes, deformation was seen along with seismic activity at Strandline Lake that is thought to be of magmatic origin (reference 17).

We do not consider the timing of activity relative to eruptions. For example, deformation recorded in Table 2 and Table S1 with an AIL = 1 or 2 does not have to occur during the eruption—it could occur at any time during the evaluation period. Also, some eruptions were not instrumentally recorded and thus do not have AIL = 3 in any category (see Section 4.4 and Table 1 in Cameron et al., 2018). Every observation of activity includes a reference, either to one or more citations in the scientific literature (Tables 2 and 3, Tables S1 and S2) or to the methods used to make this identification. Due to space limitations, we cannot cite every reference for every volcano but have cited sources that document different levels of activity.

We find that 96 of the 161 US volcanoes (59%) have at least one type of detected activity (AIL > 0). Each individual technique measured activity at between 47 and 71 volcanoes, with degassing having the most detections and deformation having the least (Table 4; Figure 2a). Most common are low levels of volcanic activity—the groups with AIL = 0 (66 or 41%) and AIL values from 0.5 to 6 (72 or 45%) make up 86% of the

Table 4
Number of Volcanoes With Detections of Activity for Each Type of Monitoring Data for This Study (See Figure 2a) and From Ewert et al. (2018)

Measurement type	# volcanoes with measured activity (AIL>0, this study; 1978–2020)	# volcanoes with measured activity by Ewert et al. (2018)
Seismic	64	77[a]
Deformation	47	31
Gas or thermal[b]	87	90
Degassing	71 (12 of these have AIL = 0.5)	N/A[b]
Thermal	67	N/A[b]
Total	96	102

Abbreviation: AIL, Activity Intensity Level.
[a]While Ewert et al. (2018) included a rank of 0.5 for volcanoes without seismic monitoring, we do not include those volcanoes here. [b]Ewert et al. (2018) grouped gas and thermal into a single category, so for comparison we both group them together and list them separately.

total (Figure 2c). There are 23 volcanoes with summed AIL values >6 that make up the remaining 14%. In the following sections, we discuss the eruption/noneruption detections, the different contributions of satellite and ground-based observations, the role of surficial and anthropogenic deformation, and the new medium-spatial resolution TIR results from the ASTER satellite.

3.1. Detections at Eruptive Volcanoes

Eruptive detections are assigned the highest AIL value of 3 for each monitoring type; eight volcanoes have the maximum summed AIL of 12 (Kīlauea, Mount St. Helens, Okmok, Redoubt, Anatahan, Veniaminof, Mauna Loa, and Augustine). These eight volcanoes have had some of the largest eruptions during the 1978–2020 period in terms of erupted volume and/or Volcano Explosivity Index (VEI); however, large eruptions (VEI = 4) at Kasatochi (2008) and Spurr (1992) did not have AIL = 3 in all categories. In fact, 23 out of the 31 volcanoes with eruptions do not have an eruptive AIL = 3 in every monitoring category (Table 2 and Table S1). While all eruptions should have thermal and gas emissions, these are only included in the table if they have been directly measured. There

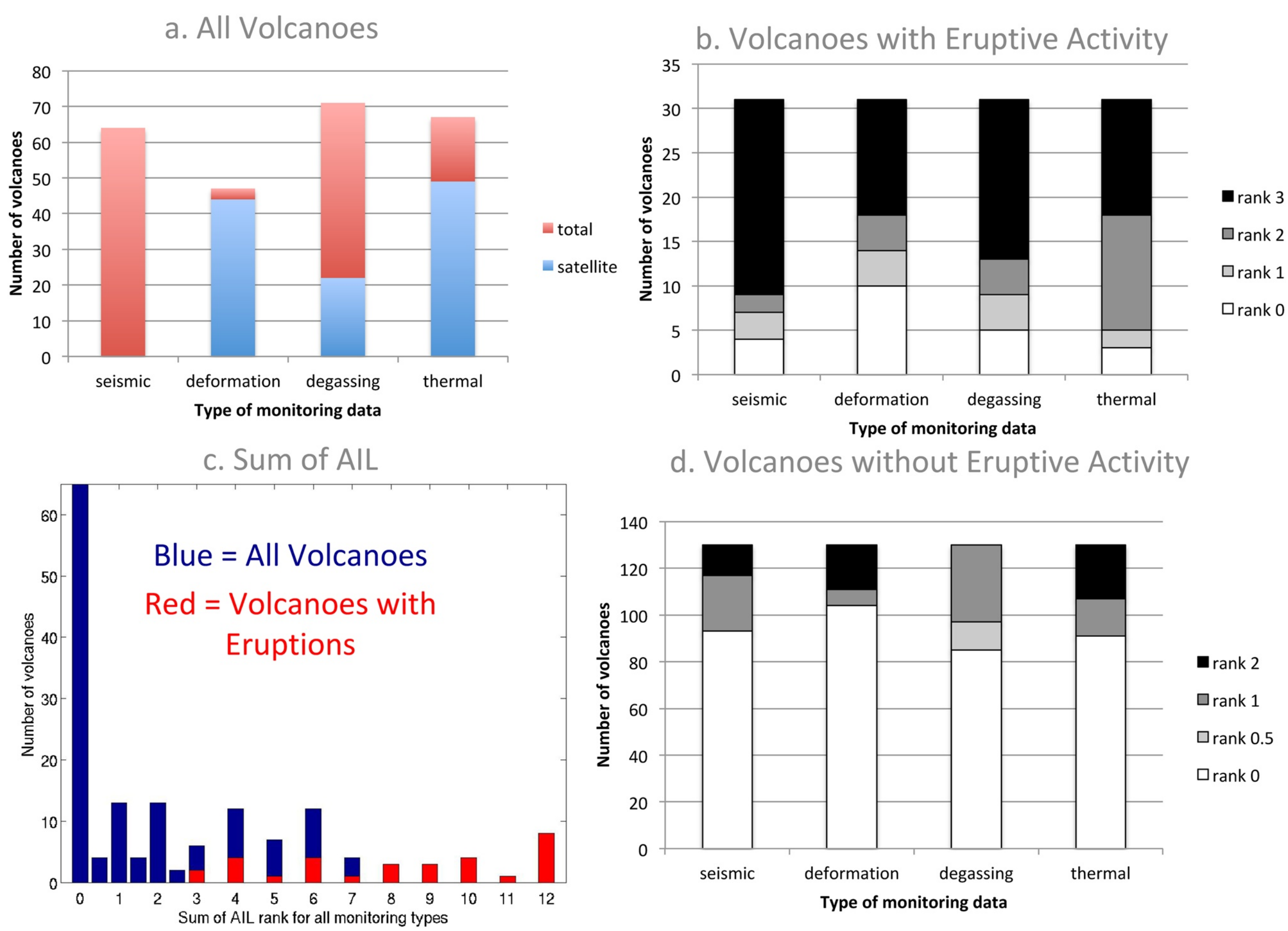

Figure 2. Histograms showing characteristics of volcano activity and detections from Tables S1 and S2. (a) Number of volcanoes with satellite detections and total detections of activity for all monitoring techniques (see Table 4 for numeric values). (b) The Activity Intensity Level (AIL) for volcanoes with eruptive activity (Table 2 and Table S1) as a function of monitoring data type. (c) The number of volcanoes with each sum of AIL for the entire population and those with detected eruptive activity. (d) The AIL for volcanoes without eruptive activity (Table S2; abridged in Table 3) as a function of monitoring data type.

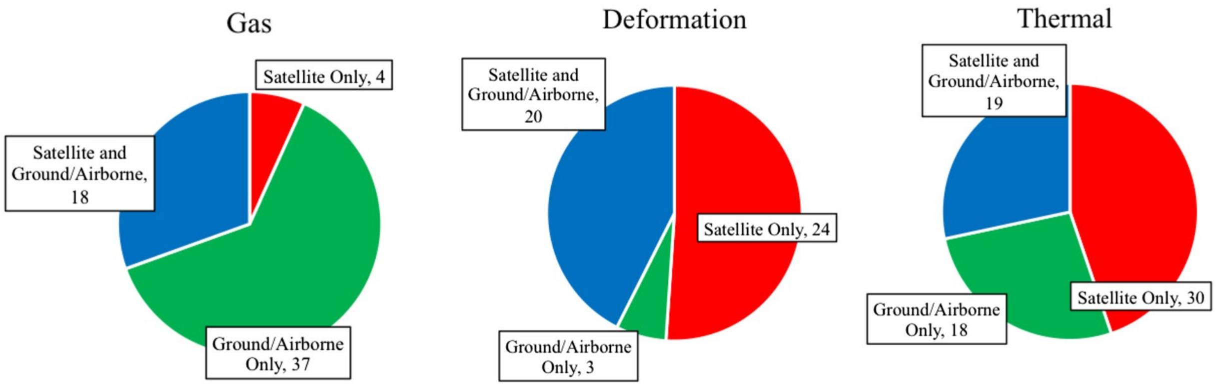

Figure 3. Pie charts for all 95 volcanoes with detectable activity illustrating the number of different types of detections from satellite, ground/airborne, or both types of measurements. The gas pie chart does not include the 12 volcanoes with Activity Intensity Level (AIL) = 0.5.

are two primary reasons for eruptive-level AIL not being detected: (a) the activity was not present and (b) a lack of suitable observations. In the cases of small eruptions, signals may be below instrument detection limits or hidden by clouds (Section 4.4). Seismic monitoring is most likely to measure eruptive AIL = 3 while deformation and thermal are the least likely (Figure 2b). Several volcanoes on this eruptive list have AIL = 0 in one or more categories. The missed detections and efficacy of different techniques are discussed in more detail in Section 4.4.

3.2. Detections at Noneruptive Volcanoes

There are 130 volcanoes in the US with the potential for volcanic activity but that do not have any eruptive activity during the study period (Table S2). Sixty-four of these volcanoes have volcanic activity that has been detected with at least one monitoring type given status quo capabilities (Table 3). For example, Seguam has satellite-detectable thermal and deformation activity but no detected seismic or degassing activity—this is not surprising considering there is no seismic network on Seguam and the nearest seismic network on Atka/Korovin ~100 km west only became operational in 2004, after the most recent Seguam eruption. At the present time, thermal monitoring is the most likely method to detect activity (Figure 2d). Finally, 66 of these volcanoes have no detectable volcanic activity (although Hualālai has surficial deformation not related to active magmatism [Poland, 2010] and Yunaska had a subsiding lava flow [Lu & Dzurisin, 2014]). This does not mean that there is no activity present at these 66 volcanoes, but rather that any activity is below the detection limit of satellite sensors and/or the volcanoes lack the necessary ground-based instrumentation for detection (Section 4.3), or that activity occurred prior to 1978, when our survey begins.

3.3. Advantages of Combining Ground-, Airborne-, and Satellite-Based Monitoring

When monitoring volcanoes, combining ground, airborne, and satellite techniques provides the most comprehensive view of activity, as these types of monitoring offer different temporal and spatial resolutions and thresholds of detection depending on the type of activity being detected (Figure 3). Seismic activity can only be detected from ground instrumentation, whereas the other three types of activity are detected though a combination of in situ and remote instruments. The majority of thermal detections are made solely by satellites (30) with 18 volcanoes observed only through ground/airborne monitoring and 19 volcanoes observed by both ground and spaceborne instruments. Conversely, the majority of detections of volcanic gas emissions (37) were made through nonsatellite observations (i.e., ground/airborne), while 18 eruptive detections of volcanic gas emissions were made by both ground/airborne and satellite detections, and only 4 volcanic gas detections observed by satellite alone (Bogoslof, Kasatochi, South Sarigan, and Chiginigak). Finally, the majority of volcanic deformation detections (24) were made by satellite, with 20 detections made by both satellite and ground/airborne sensors and only 3 detections were made by ground/airborne alone (at Mt. Baker, Anatahan, and Redoubt). Considering all monitoring techniques, 63 volcanoes have activity detected by satellite (with or without ground-based detections). The remaining 32 volcanoes have activity detected only by ground-based sensors—two of these volcanoes had eruptive activity but were submarine and thus difficult to detect by satellite (Section 4.4).

When interpreting these numbers, it is critical to consider the synergy among ground, airborne, and satellite monitoring. There are several reasons why there are four satellite-only detections for gas and three volcanoes where deformation is only detected by ground/airborne sensors. Satellites only detect degassing if there is a large volume emitted, so low-level degassing is only detected from the ground or aircraft. Satellite detection and monitoring of degassing is, at present, effectively limited to sulfur dioxide. The detection thresholds depend on sensor characteristics, vent elevation, ambient atmospheric conditions, latitude, among other parameters, and have varied with time and latitude. For ground deformation, most volcanoes do not have ground-based measurements, so satellite observations are the only data available for some volcanoes (although usually only during snow-free conditions). In recent years, satellite detections have often been used to inform ground monitoring for volcanic gas or ground deformation, and vice versa. Further, it is important to consider that only ground or satellite observations may be available at certain volcanoes during critical times. For example, only ground observations were able to measure surface deformation at eruptions before about 1991 (as a consequence, the 1984 Mauna Loa eruption could only be observed by ground-based deformation monitoring), while both ground-based and satellite InSAR have measured ground deformation since 1991 (although both data sets are not available at all volcanoes; see Lu & Dzurisin, 2014). Similarly, satellite thermal observations before 2000 (when MODIS and ASTER sensors went into orbit) were limited.

3.4. Nonmagmatic Deformation

Not all deformation detections made on or around volcanic edifices are directly related to subsurface magmatic processes. Some examples include deformation related to near surficial processes (e.g., lava flow cooling, flank creep, and faulting) as well as human activities in volcanic areas, like pumping/injection at geothermal power plants. We record with a Y/N column (Tables 2 and 3) whether this type of deformation (nonmagmatic and/or anthropogenic) has been detected. If this type of deformation is the only type of deformation recorded, the AIL = 0; however, it is much more common that this type of deformation occurs in addition to other types of subsurface activity (i.e., AIL > 0). It is important to account for surficial or anthropogenic deformation so that it is not mistakenly identified as volcanic activity, especially by ground measurements or partially coherent InSAR observations that are spatially restricted and do not measure the entire deformation pattern. We identify 20 volcanoes with this type of deformation (13 eruptive and 7 noneruptive volcanoes), with most of the deformation related to subsiding lava flows, but with at least three geothermal power plants also contributing (at Coso, Salton Buttes, and Long Valley, all in California).

3.5. New ASTER Satellite Thermal Observations

Before undertaking this study, we were only able to find 17 volcanoes in the US with peer-reviewed published thermal detections by satellite, although others were known from surveillance work by volcano observatories and others. We systematically surveyed 152 US volcanoes (we excluded submarine volcanoes and added in a few others, so the total is not 161, see Table S3) with the 90 m/pixel ASTER satellite TIR imagery. We found 47 volcanoes with satellite-detectable activity (Table S3) during 2000–2020 using ASTER, bringing the total number of volcanoes with satellite thermal detections to 49 in the 1978–2020 time frame. For the 30 volcanoes with satellite-detected thermal features documented here for the first time, we include an example ASTER image for each volcano in Figures S1–S30.

While we focused here only on whether the volcanoes had a satellite-detected thermal signal or not, we hope future work can investigate how temperature changes with time. The amount of ASTER data available for such work varies by volcano during 2000–2020. Of the US volcanoes, the most nighttime images were acquired at Kīlauea (>600), but some volcanoes had only a few acquisitions (Semisopochnoi had two); the average number was 164 over 20 years or 8.2 images/year. The number of cloud-free scenes, however, is less than this and varies from region to region (Figure 4) depending on local climatic conditions. The percentage of nighttime images that are cloud-free ranges over an order of magnitude from single digits at some Aleutian volcanoes (e.g., Okmok, Alaska, has 7% cloud-free images) to >70% in eastern California (e.g., Long

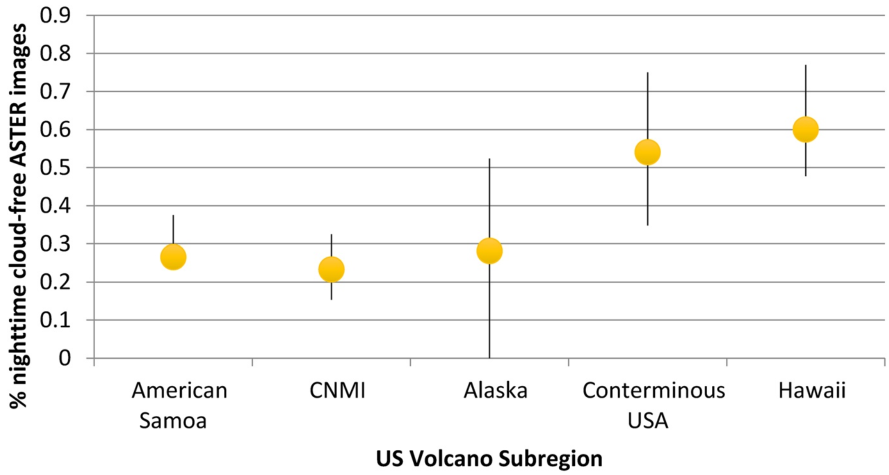

Figure 4. Percentage of nighttime cloud-free Thermal Infrared images for different US volcano subregions from the ASTER sensor on the Terra satellite between the years 2000 and 2020 (see Table S3). The yellow circle shows the average value and the line shows the minimum and maximum values for each region. CNMI is the Commonwealth of the Northern Mariana Islands.

Valley is 74%) and at Mauna Kea and Mauna Loa, Hawai‘i. Future work will aim to create time series of temperature at the 50 or so volcanoes with sufficient data using the ~20 years of available ASTER imagery (2000–2020), similar to what has been done in Latin America (Reath, Pritchard, Moruzzi, et al., 2019). In Section 4.3, we describe the limited prospects for continuing analysis using data similar to ASTER in the future.

4. Discussion

4.1. Comparison With Previous Work

As part of a comprehensive assessment of volcanic threat in the US, Ewert et al. (2018) created a supplementary table that noted whether each of 161 volcanoes considered by the report had seismic, deformation, or gas/thermal detections (they grouped gas and thermal emissions into a single category). Ewert et al. (2018) considered detected activity (what they called "historical unrest factors") as one of 24 factors in a hazard and exposure matrix when creating the US Threat Rankings shown in Tables 2 and 3, Tables S1 and S2. The period considered by Ewert et al. (2018) was unconstrained, while the period of this work was limited to 1978–2020. Considering that Ewert et al. (2018) have three monitoring categories for each volcano, there are a total of 483 activity classifications to compare with our analysis. In the Ewert et al. (2018) study, there was only a classification of whether activity was detected or not—which we can compare to our assessments of AIL > 0 or AIL = 0. We find that our assessments of volcanic activity correlate with 433 (~90%) of the 483 activity classifications by Ewert et al. (2018). They found 102 volcanoes with detected activity, while this work documents 96 volcanoes with detected activity. The differences in volcanic activity classification between the Ewert et al. (2018) study and our work are due to the different criteria, data sets, and time period. Of the 50 differences found, 26 were associated with detections only reported by Ewert et al. (2018) and 24 were associated with detections made only through our analysis. These differences are highlighted with red numbers in Tables S1 and S2.

Table 4 shows how the detections vary by monitoring technique—Ewert et al. (2018) have more detections by seismic and degassing/thermal, and we have more detections for deformation. Detections made solely by our study are explained by the inclusion of new data sets (e.g., medium-spatial resolution ASTER thermal satellite monitoring), new instruments and observations (e.g., Dzurisin et al., 2019, field observations), and the expansion of the definition of deformation activity (e.g., we consider uplift and subsidence while Ewert et al., 2018 only included uplift). Detections made solely by Ewert et al. (2018) can be attributed to the fact that their observations are not restricted to 1978–2020 and differences in the definition of what is

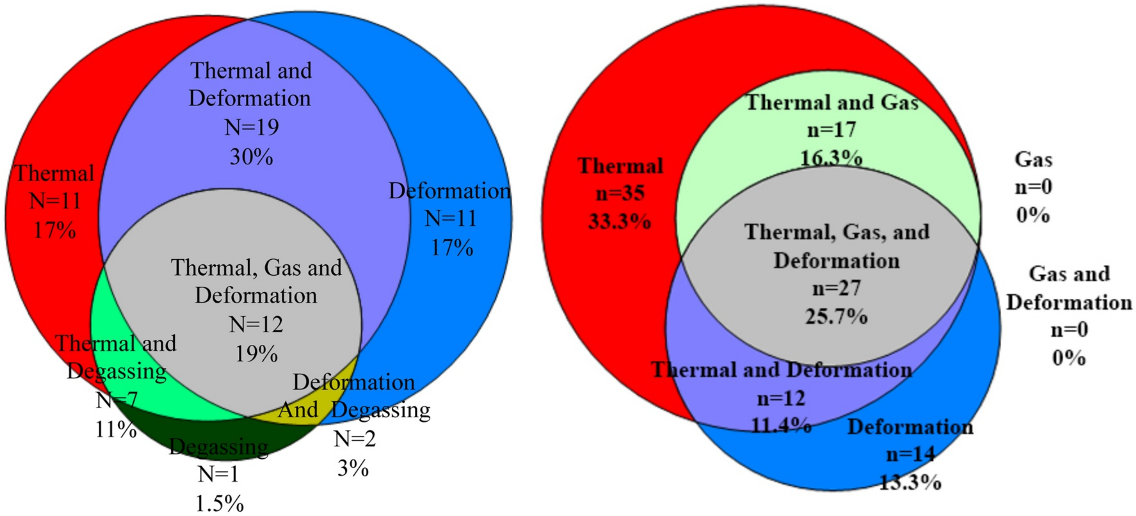

Figure 5. The types and number of measured volcanic activity identified at (a) US ($N = 63$) and (b) Latin America volcanoes ($N = 105$). (b) Based on data from Reath, Pritchard, Poland, et al. (2019).

considered seismic volcanic activity (i.e., distal volcano-tectonic events without a clear volcanic origin). In summary, we see our results as confirming and building on the work of Ewert et al. (2018) by adding new data sets and providing more granularity through the AIL ranking. The differences in our results are mostly related to volcanoes where there are ambiguous signs of activity, for example, seismic or deformation activity in areas with closely spaced volcanoes where distal VTs and offset deformation sources (e.g., Lerner et al., 2020) could correspond to two or more volcanoes (e.g., places on the Alaska Penninsula, Tanaga Island, Atka/Korovin, calderas with multiple stratocones on and adjacent to the caldera). If a particular volcano could not be singled out as hosting the activity, Ewert et al. (2005, 2018) allowed it to be counted toward the score of nearby possible systems. More detailed analyses are needed to assess the detections at these volcanoes (see Section 4.3).

To put the number of satellite detections of volcanic activity in context, we note that the most thorough available compilation of US eruptive and noneruptive volcanic activity is by Diefenbach et al. (2009), updated by Ewert et al. (2018). They summarized volcanic eruptions and unrest at Holocene volcanoes in the US from 1980 to 2017: 44 volcanoes produced 120 eruptions and 45 episodes of unrest. Diefenbach et al. (2009) defined "unrest episodes based on the criterion that a volcano observatory responded in some way to each episode listed in this report." By these criteria, most of the activity documented at the 96 volcanoes in Tables 2 and 3, Tables S1 and S2 would not be considered unrest. With the AILs reported here, there are now baseline measurements at more volcanoes against which any departures from normal background levels can be gauged with expanded ground-based and satellite data (Section 4.3).

4.2. Comparison With Other Regions

We are not aware of any other country or region that has a similar compilation of space and ground-based multiparameter observations of volcanic activity to what is available for the US in Tables S1 and S2. We encourage efforts to make multiparameter compilations easier to create and access (e.g., World Organization of Volcano Observatories database: Newhall et al., 2017). The best comparison we can make is to a compilation of global volcano satellite observations in Poland et al. (2019). The US has the most volcanoes (63, 39% of 161 volcanoes) with satellite-detected activity (with or without ground-based detections), followed by Indonesia (45, 32% of volcanoes from VOTW), Chile (40, 38%), Japan (27, 24%), and Russia (24, 17%). The distribution of detections among monitoring types is also different in different regions. In Figure 5, we compare the US satellite detections (with or without ground detections as well) having $N = 63$ out of 161 volcanoes, with those from Latin America ($N = 105$ out of 330) (Furtney et al., 2018; Pritchard et al., 2018; Reath, Pritchard, Moruzzi, et al., 2019; Reath, Pritchard, Poland, et al., 2019).

In Latin America, 31% of the volcanoes have satellite-detected activity, compared to 39% of US volcanoes. Although it is possible that the volcanoes in the US have fundamentally different activity levels than in Latin America, they both share similar, but not identical, populations. Both have a mix of arc and hotspot volcanism (including oceanic islands like Hawaii and the Galápagos), span a range of tropical to semiarid to subpolar regions with varying cloud cover (Figure 4 and Reath, Pritchard, Moruzzi, et al., 2019), and have similar normalized eruption rates between 1978 and 2020 (152 eruptions in the US for 161 volcanoes compared to 314 eruptions at 330 volcanoes in Latin America according to VOTW). Instead, our hypothesis is that activity is underreported at Latin American volcanoes. While similar types of satellite data are used to study US and Latin American volcanoes, there are more ground-based instruments at US volcanoes (e.g., Brown et al., 2015), which could prompt more focused satellite observations. For example, satellite thermal observations are the only type of activity measured at 33% of Latin American volcanoes but only 17% at US volcanoes. We suspect that these volcanoes in Latin America with satellite thermal activity also have some other type of activity (gas emissions or deformation) that has been missed due to limited field observations and/or monitoring networks.

4.3. Incompleteness of Our Compilation

The US has 96 volcanoes with detected activity, but there are several reasons to believe that this number is an underestimate. Ground-based detections of volcanic activity rely on placing sensors close to the source of the activity, and it is well known that certain US volcanoes lack sufficient ground-based monitoring (e.g., Ewert et al., 2005; Moran et al., 2008). One indication of the lack of ground-based degassing observations is that eight subaerial and four primarily submarine US volcanoes have AIL rank 0.5, meaning that degassing activity has been visually observed but has not yet been quantified. Although thermal, degassing, and deformation activity can be measured through satellite remote sensing, the available satellite data also have limits (Poland et al., 2020). Satellite observations do not have sufficient resolution to see quiescent degassing at most US volcanoes and satellite techniques are most suited to measure SO_2, which may not be degassing at many volcanoes, especially those with mixed magmatic-hydrothermal systems. Our analysis of medium-spatial resolution (90 m/pixel) satellite thermal data has increased the number of satellite detections at US volcanoes by ∼175% (47 known now compared to 17 from previous work), but we wonder how many more volcanoes would be added if spatial resolution were increased by another order of magnitude. For example, higher-spatial resolution satellite observations of volcanic ash resulted in increased detections of less significant activity (Engwell et al., 2021). Further, we have recorded how the number of acquisitions and percentage of cloud-free ASTER scenes varies for each volcano in Table S3 and Figure 4; thus, our ability to detect thermal activity also varies among volcanoes. Finally, the spatial and temporal variations in the quality of satellite InSAR monitoring of ground deformation at US volcanoes are discussed in several publications (e.g., Dzurisin et al., 2019; Lu & Dzurisin, 2014). While satellites both currently in orbit and planned will increase our ability to monitor ground deformation, thermal emissions, and degassing of US volcanoes from space, observation gaps are also expected. Specifically, the available medium-spatial resolution TIR sensors (e.g., ASTER) are near the end of their missions, and a gap in such data in the future is a near certainty (e.g., National Academies of Sciences, Engineering, and Medicine, 2018). These satellite observations are essential for monitoring the subtle thermal features at ∼29% of US volcanoes.

We suspect that for some volcanoes, the AIL is an underestimate due to a lack of suitable observations for all types of volcanic activity. In Section 4.4, we discuss the underestimate of AIL for eruptions, but this applies to noneruptive activity as well. Discrepancies in the AIL rank among monitoring techniques at a given volcano can be a useful tool to target new deployments of certain types of ground-based sensors, prioritize field campaigns and/or to focus analysis on one or more type(s) of satellite data. For example, Veniaminof, Baker, Shishaldin, and Cleveland have low levels of seismic monitoring but high AIL scores. Similarly, Takawangha and Kupreanof have high summer AIL scores but degassing AIL of 0 and 0.5, respectively, indicating that focused ground-based measurements would provide a more complete picture of background activity at these moderate to very high threat (Ewert et al., 2018) volcanoes.

4.4. Missed Detections During Eruptive Events

As AIL = 3 in the classification system is reserved for detections made during a volcanic eruption, it stands to reason that all volcanoes with an eruption should have AIL = 3 values across the board. However, this is not the case—only 8 of 31 volcanoes in Table 2 have AIL = 3 detections for every type. Further, seven volcanoes with confirmed eruptions in the VOTW catalog (but not necessarily in the AVO catalog) between 1978 and 2020 (Akutan, Makushin, Seguam, Chiginagak, Amukta, Kiska, and Gareloi) do not have any AIL = 3. It is important to note that since 2002, no eruption at a US volcano has been completely missed when all types of monitoring data are considered (Cameron et al., 2018)—although there were multiple eruptions that were detected after they occurred and not in real time. Volcanoes that are missing AIL = 3 for one or more monitoring technique during eruption fall into four categories:

1. Submarine volcanoes (e.g., South Sarigan Seamount, Ahyi Seamount, and Ruby): submarine eruptions are, by their nature, difficult to monitor. Satellite sensors cannot identify activity occurring underneath the ocean, although the largest submarine eruptions produce gas emissions that can be detected on the surface of the ocean (e.g., South Sarigan Seamount) or seismic signals large enough to be detected by nearby stations (e.g., Ahyi Seamount and Ruby).
2. Volcanoes with short eruptive periods and/or cloudy conditions: For thermal and degassing detections, eruptive activity can be missed by satellites if the eruption is low intensity or the volcano is cloud covered—this is especially likely at eruptions that only last a few days or weeks in the often cloud-covered Aleutian arc (Figure 4). These types of eruptions can still be detected with ground-based seismic and infrasound observations (Coombs et al., 2018; De Angelis et al., 2012). To detect the thermal and degassing emissions from these eruptions, ground and airborne sensors are needed. Satellites that can make frequent high- to medium-spatial resolution measurements could also exploit breaks in the clouds.
3. Volcanoes that did not produce a detectable level of activity in a certain type of monitoring data: For example, Lu and Dzurisin (2014) argue that the lack of ground deformation associated with eruptions at Shishaldin, Cleveland, and Pavlof volcanoes (all listed in Table 2) is because these are open-conduit stratovolcanoes "where magma rises freely and rapidly shortly before and during eruptions, causing little or no surface deformation." To detect deformation at these types of volcanoes requires ground-based sensors near the edifice and/or high spatial and temporal resolution InSAR measurements (e.g., Salzer et al., 2014). Nine eruptions lack an AIL = 3 for seismic monitoring due to a lack of close-by instruments (Pagan, Makusin, Kiska, Seguam, Gareloi, Amukta, Chiginagak, Akutan, and Westdahl). There are 17 volcanoes that have an AIL rank less than 3 for degassing and thermal emissions (Table 2 and Table S1)—we suspect that there were such emissions during the eruption, but that they could not be detected from space (see explanations in categories 2 and 4).
4. Older eruptions when there were not sufficient satellite data available. Some of these eruptions may fall into categories 1–3 above, but there are also some significant eruptions, like Westdahl (VEI 3 in 1991–1992, e.g., Lu & Dzurisin, 2014) where neither gas or thermal coeruptive emissions were detected. Westdahl emitted lava and would be detectable with currently available satellite thermal and gas observations.

5. Conclusions

We have developed a compilation of detected volcanic activity in the US that focuses not just on eruptions and unrest, but any type of instrumentally recorded observations. We integrate multiple types of satellite and ground-based data to quantify the level of activity through the AIL. This simple ranking provides a metric to compare measured activity levels across four types of monitoring data and volcanoes with different background activity levels. Background activity at some volcanoes have AIL>0. AIL can be used to help prioritize future measurements or analysis when considered in a larger context of risk-mitigation or scientific objectives. Volcanoes with high summed AIL scores that have a low AIL in one or more monitoring category could be good targets for enhanced monitoring—such as increased seismic monitoring at Veniaminof, Baker, Shishaldin, and Cleveland, and gas emission observations at Takawangha and Kupreanof.

The AIL is not a perfect metric—for example, future work should include actual temperature measurements and gas fluxes instead of the current ranking based on whether the thermal and degassing signals are large enough (or not) to be seen from space. All monitoring techniques are equally weighted in the summed AIL, but some types of monitoring data should be more heavily weighted if they strongly correlate with future eruptive activity. Similarly, recent activity should be weighted more heavily than older activity. Further, an improved AIL would account for changes in activity and detection threshold over time and would record whether measured activity levels from the different techniques were coincident, within a few years, or made decades apart. In the future, changes in AIL could be automatically detected using deep learning and other techniques (e.g., Anantrashirchai et al., 2018) and applied to other regions.

Our key conclusions are as follows:

1. Out of the 161 US volcanoes analyzed, 96 were found to have detectable volcanic activity from ground-based seismic monitoring and/or ground-, air-, and space-based measurements of gas and thermal emissions, or ground deformation. The majority of the detected activity is not related to eruptions or unrest and serves as a baseline to compare against future episodes of increased activity. Although a significant fraction of US volcanoes have some type of detected activity (59%), we suspect that this is a lower bound. Many volcanoes have limited or no ground-based observations, and the available satellites may not be able to detect low levels of activity. For example, gas and thermal emissions for certain eruptions will be missed if there are clouds and the eruption is short lived. Also, there are 12 volcanoes with a degassing AIL of 0.5, indicating that degassing has been observed visually but not quantified.
2. We document dozens of volcanoes where volcanic activity is only measured by satellite (especially for thermal observations) and dozens of other volcanoes where only ground-based sensors have detected activity (e.g., seismic and degassing observations). One goal of our analysis was to show that multiparameter satellite data are one of the most effective tools for monitoring volcanoes and to overcome the perception that the capabilities of satellites are not widely known (Bally, 2012). We suspect that, for many volcanoes around the world, the data are not always acquired with the proper spatial and/or temporal resolution. For example, the difference in the percentage of US volcanoes with activity detected by satellite (39%) compared to Latin American volcanoes (31%) could be related to insufficient satellite observations in Latin America. Our work confirms that satellite- and ground-based data must be used together to provide sufficient spatial and temporal coverage and sensitivity for US volcanoes.
3. We find previously undocumented volcanic thermal activity at 30 volcanoes using medium-spatial resolution (90 m/pixel) satellite imagery from ASTER acquired during 2000–2020. These satellite detections account for 45% of the 67 US volcanoes with detected thermal activity. On the other hand, satellite thermal data are not being fully exploited—medium resolution TIR data are not acquired regularly at some volcanoes and some satellites acquire few nighttime images (e.g., Landsat-8 and Sentinel-2). Many US volcanoes are only covered by a handful of cloud-free nighttime medium-spatial resolution (<100 m/pixel) TIR images per year (Table S3). Our work demonstrates the need for continuing and densifying the time series of high- to medium-spatial resolution nighttime satellite TIR observations to track thermal activity and exploring the use of higher-spatial resolution TIR satellite data sets.
4. We document that ground deformation not associated with ongoing magmatic activity is widespread and must be considered when assessing the origin of ground deformation in volcanic areas. Twenty volcanoes in the US have ground deformation associated with surficial processes (e.g., lava flow subsidence or faulting) or human activities from geothermal energy production.

Data Availability Statement

This project did not generate any new data.

Acknowledgments
The idea for this paper was born at the 2019 workshop of the Volcano Remote Sensing Working Group supported by the John Wesley Powell Center for Analysis and Synthesis, funded in part by the US Geological Survey; the authors thank Jill Baron and Leah Colasuonno for facilitating this working group. Work on the paper began and grew in new directions during the 2019 CIDER summer program on volcanoes at the University of California Berkeley; the authors thank the program for financial support and the organizers and participants in that program for creating a stimulating environment. M. E. Pritchard was partly supported by NASA grant 80NSSC21K0842. The authors thank John Ewert, Freysteinn Sigmundsson, Larry Mastin, and Robert Wright for critical reviews.

References

Alaska Volcano Observatory. (2021). *Catalog of eruptions at Alaskan volcanoes*. Retrieved from https://avo.alaska.edu/volcanoes/erupt-search.php

Amelung, F., Yun, S.-H., Walter, T. R., Segall, P., & Kim, S.-W. (2007). Stress control of deep rift intrusion at Mauna Loa volcano, Hawaii. *Science*, *316*(5827), 1026–1030. https://doi.org/10.1126/science.1140035

Anantrasirichai, N., Biggs, J., Albino, F., Hill, P., & Bull, D. (2018). Application of machine learning to classification of volcanic deformation in routinely generated InSAR data. *Journal of Geophysical Research: Solid Earth*, *123*, 6592–6606. https://doi.org/10.1029/2018JB015911

Baker, E. T., Embley, R. W., Walker, S. L., Resing, J. A., Lupton, J. E., Nakamura, K. I., et al. (2008). Hydrothermal activity and volcano distribution along the Mariana arc. *Journal of Geophysical Research*, *113*, B08S09. https://doi.org/10.1029/2007JB005423

Bally, P. (Ed.). (2012). *Scientific and technical memorandum of the international forum on satellite EO and geohazards*. https://doi.org/10.5270/esa-geo-hzrd-2012

Banks, N. G., Koyanagi, R. Y., Sinton, J. M., & Honma, K. T. (1984). The eruption of Mount Pagan Volcano, Mariana Islands, 15 May 1981. *Journal of Volcanology and Geothermal Research*, *22*(3–4), 225–269.

Bergfeld, D., Evans, W. C., Howle, J. F., & Farrar, C. D. (2006). Carbon dioxide emissions from vegetation-kill zones around the resurgent dome of Long Valley caldera, eastern California, USA. *Journal of Volcanology and Geothermal Research*, *152*(1–2), 140–156. https://doi.org/10.1016/j.jvolgeores.2005.11.003

Bergfeld, D., Evans, W. C., Hunt, A. G., Lopez, T., & Schaefer, J. R. (2020). A post-eruption study of gases and thermal waters at Okmok volcano, Alaska. *Journal of Volcanology and Geothermal Research*, *396*, 106853. https://doi.org/10.1016/j.jvolgeores.2020.106853

Bergfeld, D., Lewicki, J. L., Evans, W. C., Hunt, A. G., Revesz, K., & Huebner, M. (2013). *Geochemical investigation of the hydrothermal system on Akutan Island, Alaska, July 2012* (U.S. Geological Survey Scientific Investigations Report 2013-5231, p. 19). https://doi.org/10.3133/sir20135231

Brown, S. K., Loughlin, S. C., Sparks, R. S. J., & Vye-Brown, C. (2015). *Global volcanic hazards and risk: Technical background paper for the Global Assessment Report on Disaster Risk Reduction 2015*. Global Volcano Model and IAVCEI. https://doi.org/10.1007/s13398-014-0173-7.2

Brumbaugh, D. S., Hodge, B. E., Linville, L., & Cohen, A. (2014). Analysis of the 2009 earthquake swarm near Sunset Crater volcano, Arizona. *Journal of Volcanology and Geothermal Research*, *285*, 18–28. https://doi.org/10.1016/j.jvolgeores.2014.07.016

Cameron, C. E., Dixon, J. P., Neal, C. A., Waythomas, C. F., Schaefer, J. R., & McGimsey, R. G. (2017). *2014 volcanic activity in Alaska—Summary of events and response of the Alaska Volcano Observatory* (U.S. Geological Survey Scientific Investigations Report 2017-5077, p. 81). https://doi.org/10.3133/sir20175077

Cameron, C. E., Prejean, S. G., Coombs, M. L., Wallace, K. L., Power, J. A., & Roman, D. C. (2018). Alaska Volcano Observatory alert and forecasting timeliness: 1989–2017. *Frontiers of Earth Science*, *6*, 86. https://doi.org/10.3389/feart.2018.00086

Cameron, C. E., Schaefer, J. R., & Ekberg, P. G. (2020). *Historically active volcanoes of Alaska: Alaska Division of Geological and Geophysical Surveys Miscellaneous Publication 133 v. 4, 2 sheets*. https://doi.org/10.14509/30426

Cameron, C. E., & Snedigar, S. F. (2016). *Alaska Volcano Observatory Image Database: Alaska Division of Geological and Geophysical Surveys Digital Data Series 13*. https://doi.org/10.14509/29689

Caplan-Auerbach, J., & Prejean, S. G. (2005). High levels of non-eruptive seismicity at Mount Gareloi Volcano, Alaska. *Eos, Transactions American Geophysical Union*, *86*(52).

Carn, S. A., Clarisse, L., & Prata, A. (2016). Multi-decadal satellite measurements of global volcanic degassing. *Journal of Volcanology and Geothermal Research*, *311*, 99–134. Retrieved from http://www.sciencedirect.com/science/article/pii/S0377027316000032

Carn, S. A., Fioletov, V. E., McLinden, C. A., Li, C., & Krotkov, N. A. (2017). A decade of global volcanic SO_2 emissions measured from space. *Scientific Reports*, *7*, 44095. https://doi.org/10.1038/srep44095

Carn, S. A., Krueger, A., Arellano, S., & Krotkov, N. (2008). Daily monitoring of Ecuadorian volcanic degassing from space. *Journal of Volcanology and Geothermal Research*, *176*(1), 141–150. Retrieved from http://www.sciencedirect.com/science/article/pii/S0377027308000619

Carn, S. A., Krueger, A. J., Bluth, G. J. S., Schaefer, S. J., Krotkov, N. A., Watson, I. M., & Datta, S. (2003). Volcanic eruption detection by the Total Ozone Mapping Spectrometer (TOMS) instruments: A 22-year record of sulphur dioxide and ash emissions. *Geological Society, London, Special Publications*, *213*(1), 177–202. https://doi.org/10.1144/GSL.SP.2003.213.01.11

Casadevall, T., Rose, W., Gerlach, T., Greenland, L. P., Ewert, J., Wunderman, R., & Symonds, R. (1983). Gas emissions and the eruptions of Mount St. Helens through 1982. *Science*, *221*(4618), 1383–1385.

Chouet, B. A., Page, R. A., Stephens, C. D., Lahr, J. C., & Power, J. A. (1994). Precursory swarms of long-period events at Redoubt Volcano (1989–1990), Alaska: Their origin and use as a forecasting tool. *Journal of Volcanology and Geothermal Research*, *62*(1–4), 95–135.

Christenson, B. W., Kennedy, B. M., Adams, M. C., Bjornstad, S. C., & Buck, C. (2007). *Chemical and isotopic characteristics of the Coso east flank hydrothermal fluids: Implications for the location and nature of the heat source*. Paper presented at Proceedings of the Thirty-Second Workshop on Geothermal Reservoir Engineering Stanford University.

Coombs, M. L., Wech, A. G., Haney, M. M., Lyons, J. J., Schneider, D. J., Schwaiger, H. F., et al. (2018). Short-term forecasting and detection of explosions during the 2016–2017 eruption of Bogoslof volcano, Alaska. *Frontiers of Earth Science*, *6*, 122. https://doi.org/10.3389/feart.2018.00122

Coppola, D., Laiolo, M., & Cigolini, C. (2016). *Enhanced volcanic hot-spot detection using MODIS IR data: Results from the MIROVA system*. Geological Society. Retrieved from http://sp.lyellcollection.org/content/426/1/181.short

Craig, H., Lupton, J. E., Welhan, J. A., & Poreda, R. (1978). Helium isotope ratios in Yellowstone and Lassen Park volcanic gases. *Geophysical Research Letters*, *5*(11), 897–900.

Crankshaw, I. M., Archfield, S. A., Newman, A. C., Bergfeld, D., Clor, L. E., Spicer, K. R., et al. (2018). Multi-year high-frequency hydrothermal monitoring of selected high-threat Cascade Range volcanoes. *Journal of Volcanology and Geothermal Research*, *356*, 24–35. https://doi.org/10.1016/j.jvolgeores.2018.02.014

Crider, J. G., Frank, D., Malone, S. D., Poland, M. P., Werner, C., & Caplan-Auerbach, J. (2011). Magma at depth: A retrospective analysis of the 1975 unrest at Mount Baker, Washington, USA. *Bulletin of Volcanology*, *73*(2), 175–189. https://doi.org/10.1007/s00445-010-0441-0

Crowell, B. W., Bock, Y., Sandwell, D. T., & Fialko, Y. (2013). Geodetic investigation into the deformation of the Salton Trough. *Journal of Geophysical Research: Solid Earth*, *118*, 5030–5039. https://doi.org/10.1002/jgrb.50347

De Angelis, S., Fee, D., Haney, M., & Schneider, D. (2012). Detecting hidden volcanic explosions from Mt. Cleveland Volcano, Alaska with infrasound and ground-coupled airwaves. *Geophysical Research Letters*, *39*, L21312. https://doi.org/10.1029/2012GL053635

DeGrandpre, K. G., Pesicek, J. D., Lu, Z., DeShon, H. R., & Roman, D. C. (2019). High rates of inflation during a noneruptive episode of seismic unrest at Semisopochnoi Volcano, Alaska in 2014–2015. *Geochemistry, Geophysics, Geosystems*, *20*, 6161–6186. https://doi.org/10.1029/2019GC008720

Dehn, J., Dean, K., & Engle, K. (2000). Thermal monitoring of North Pacific volcanoes from space. *Geology*, *28*(8), 755–758.

Dehn, J., Worden, A., & Webley, P. (2011). *Time series of North Pacific volcanic eruptions*. American Geophysical Union Fall Meeting, Abstract V53E-2677.

De Moor, J. M., Fischer, T. P., Hilton, D. R., Hauri, E., Jaffe, L. A., & Camacho, J. T. (2005). Degassing at Anatahan volcano during the May 2003 eruption: Implications from petrology, ash leachates, and SO_2 emissions. *Journal of Volcanology and Geothermal Research*, *146*(1–3), 117–138. https://doi.org/10.1016/j.jvolgeores.2004.11.034

Diefenbach, A. K., Guffanti, M., & Ewert, J. W. (2009). *Chronology and references of volcanic eruptions and selected unrest in the United States, 1980–2008* (U.S. Geological Survey Open-File Report 2009–1118, p. 85). https://doi.org/10.3133/ofr20091118

Dietterich, H. R., Poland, M. P., Schmidt, D. A., Cashman, K. V., Sherrod, D. R., & Espinosa, A. T. (2012). Tracking lava flow emplacement on the east rift zone of Kīlauea, Hawai'i, with synthetic aperture radar coherence. *Geochemistry, Geophysics, Geosystems*, *13*, Q05001. https://doi.org/10.1029/2011GC004016

Dixon, J. P., Cameron, C., McGimsey, R. G., Neal, C. A., & Waythomas, C. (2015). *2013 volcanic activity in Alaska: Summary of events and response of the Alaska Volcano Observatory* (U.S. Geological Survey Scientific Investigations Report, 2015-5110). https://doi.org/10.3133/sir20155110

Dixon, J. P., Stihler, S. D., Power, J. A., & Searcy, C. (2008). *Catalog of earthquake hypocenters at Alaskan volcanoes: January 1 through December 31, 2006* (U.S. Geological Survey Data Series, 326, p. 79). https://doi.org/10.3133/ds326

Doukas, M. P., & Gerlach, T. M. (1995). Sulfur dioxide scrubbing during the 1992 eruptions of Crater Peak, Mount Spurr Volcano, Alaska. In *The 1992 eruptions of Crater Peak vent, Mount Spurr Volcano, Alaska* (2139, pp. 47–57).

Doukas, M. P., & McGee, K. A. (2007). *A compilation of gas emission-rate data from volcanoes of Cook Inlet (Spurr, Crater Peak, Redoubt, Iliamna, and Augustine) and Alaska Peninsula (Douglas, Fourpeaked, Griggs, Mageik, Martin, Peulik, Ukinrek Maars), and. from 1995-2006* (U.S. Geological Survey Open-File Report 2007-1400). https://doi.org/10.3133/ofr20071400

Dzurisin, D. (2006). *Volcano deformation: New geodetic monitoring techniques* (pp. 441). Springer Science and Business Media.

Dzurisin, D., Lisowski, M., Wicks, C. W., Poland, M. P., & Endo, E. T. (2006). Geodetic observations and modeling of magmatic inflation at the Three Sisters volcanic center, central Oregon Cascade Range, USA. *Journal of Volcanology and Geothermal Research*, *150*(1–3), 35–54. https://doi.org/10.1016/j.jvolgeores.2005.07.011

Dzurisin, D., Lu, Z., Poland, M. P., & Wicks, C. W. (2019). Space-based imaging radar studies of U.S. volcanoes. *Frontiers in Earth Science*, *6*, 249. https://doi.org/10.3389/feart.2018.00249

Dzurisin, D., Poland, M. P., & Bürgmann, R. (2002). Steady subsidence of Medicine Lake volcano, northern California, revealed by repeated leveling surveys. *Journal of Geophysical Research*, *107*(B12), 2372. https://doi.org/10.1029/2001JB000893

Ebmeier, S. K., Biggs, J., Mather, T. A., Elliott, J. R., Wadge, G., & Amelung, F. (2012). Measuring large topographic change with InSAR: Lava thicknesses, extrusion rate and subsidence rate at Santiaguito volcano, Guatemala. *Earth and Planetary Science Letters*, *335–336*, 216–225. https://doi.org/10.1016/j.epsl.2012.04.027

Elias, T., Kern, C., Sutton, A. J., & Horton, K. (2020). *Sulfur dioxide emission rates from Kīlauea Volcano, Hawaii, 2008–2013*. U.S. Geological Survey data release. https://doi.org/10.5066/P9K0EZII

Embley, R. W., Baker, E. T., Butterfield, D. A., Chadwick, W. W., Lupton, J. E., Resing, J. A., et al. (2007). Exploring the submarine ring of fire: Mariana Arc-Western Pacific. *Oceanography*, *20*(4), 68–79. https://doi.org/10.5670/oceanog.2007.07

Embley, R. W., Baker, E. T., Chadwick, W. W., Jr., Lupton, J. E., Resing, J. A., Massoth, G. J., & Nakamura, K. (2004). Explorations of Mariana arc volcanoes reveal new hydrothermal systems. *Eos, Transactions American Geophysical Union*, *85*(4), 37–40.

Engwell, S., Mastin, L., Tupper, A., Kibler, J., Acethorp, P., Lord, G., & Filgueira, R. (2021). Near-real-time volcanic cloud monitoring: Insights into global explosive volcanic eruptive activity through analysis of Volcanic Ash Advisories. *Bulletin of Volcanology*, *83*(2), 9. https://doi.org/10.1007/s00445-020-01419-y

Evans, W. C., Bergfeld, D., McGimsey, R. G., & Hunt, A. G. (2009). Diffuse gas emissions at the Ukinrek Maars, Alaska: Implications for magmatic degassing and volcanic monitoring. *Applied Geochemistry*, *24*(4), 527–535. https://doi.org/10.1016/j.apgeochem.2008.12.007

Evans, W. C., Bergfeld, D., Neal, C. A., McGimsey, R. G., Werner, C. A., Waythomas, C. F., et al. (2015). *Aleutian arc geothermal fluids: Chemical analyses of waters and gases*. U.S. Geological Survey data release. https://doi.org/10.5066/F78G8HR1

Evans, W. C., van Soest, M. C., Mariner, R. H., Hurwitz, S., Ingebritsen, S. E., Wicks, C. W., Jr., & Schmidt, M. E. (2004). Magmatic intrusion west of Three Sisters, central Oregon, USA: The perspective from spring geochemistry. *Geology*, *32*(1), 69–72. https://doi.org/10.1130/G19974.1

Ewert, J. W. (2007). System for ranking relative threats of U.S. volcanoes. *Natural Hazards Review*, *8*(4), 112–124. https://doi.org/10.1061/(ASCE)1527-6988(2007)8:4(112)

Ewert, J. W., Diefenbach, A. K., & Ramsey, D. W. (2018). *2018 update to the U.S. Geological Survey National Volcanic Threat Assessment* (U.S. Geological Survey Scientific Investigations Report 2018-5140). https://doi.org/10.3133/sir20185140

Ewert, J. W., Guffanti, M., & Murray, T. L. (2005). *An assessment of volcanic threat and monitoring capabilities in the United States: Framework for a National Volcano Early Warning System* (Open-File Report). https://doi.org/10.3133/OFR20051164

Farrell, J., Smith, R. B., Taira, T., Chang, W.-L., & Puskas, C. M. (2010). Dynamics and rapid migration of the energetic 2008–2009 Yellowstone Lake earthquake swarm. *Geophysical Research Letters*, *37*, L19305. https://doi.org/10.1029/2010GL044605

Fialko, Y., & Simons, M. (2000). Deformation and seismicity in the Coso geothermal area, Inyo County, California: Observations and modeling using satellite radar interferometry. *Journal of Geophysical Research*, *105*(B9), 21781–21793.

Fialko, Y., & Simons, M. (2001). Evidence for on-going inflation of the Socorro magma body, New Mexico, from interferometric synthetic aperture radar imaging. *Geophysical Research Letters*, *28*(18), 3549–3552.

Fierstein, J., & Hildreth, W. (2008). Kaguyak dome field and its Holocene caldera, Alaska Peninsula. *Journal of Volcanology and Geothermal Research*, *177*(2), 340–366. https://doi.org/10.1016/j.jvolgeores.2008.05.016

Fioletov, V. E., Mclinden, C. A., Krotkov, N., Li, C., Joiner, J., Theys, N., et al. (2016). A global catalog of large SO_2 sources and emissions derived from the Ozone Monitoring Instrument. *Atmospheric Chemistry and Physics*, *16*, 11497–11519. https://doi.org/10.5194/acp-16-11497-2016

Fischer, T. P., Arellano, S., Carn, S., Aiuppa, A., Galle, B., Allard, P., et al. (2019). The emissions of CO_2 and other volatiles from the world's subaerial volcanoes. *Scientific Reports*, *9*(1), 1–11. https://doi.org/10.1038/s41598-019-54682-1

Fischer, T. P., & Lopez, T. M. (2016). First airborne samples of a volcanic plume for $\delta^{13}C$ of CO_2 determinations. *Geophysical Research Letters*, *43*, 3272–3279. https://doi.org/10.1002/2016GL068499

Friedman, J. D., Williams, D. L., & Frank, D. (1982). Structural and heat flow implications of infrared anomalies at Mt. Hood, Oregon, 1972–1977. *Journal of Geophysical Research*, *87*(B4), 2793–2803. https://doi.org/10.1029/JB087ib04p02793

Furtney, M. A., Pritchard, M. E., Biggs, J., Carn, S. A., Ebmeier, S. K., Jay, J. A., et al. (2018). Synthesizing multi-sensor, multi-satellite, multi-decadal datasets for global volcano monitoring. *Journal of Volcanology and Geothermal Research*, *365*, 38–56. https://doi.org/10.1016/j.jvolgeores.2018.10.002

Gardine, M., West, M., Werner, C., & Doukas, M. (2011). Evidence of magma intrusion at Fourpeaked volcano, Alaska in 2006–2007 from a rapid-response seismic network and volcanic gases. *Journal of Volcanology and Geothermal Research*, *200*(3–4), 192–200. https://doi.org/10.1016/j.jvolgeores.2010.11.018

Gerlach, T. M., McGee, K. A., & Doukas, M. P. (2008). Emission rates of CO_2, SO_2, and H_2S, scrubbing, and preeruption excess volatiles at Mount St. Helens, 2004–2005. In D. R. Sherrod, W. E. Scott, & P. H. Stauffer (Eds.), *A volcano rekindled—The renewed eruption of Mount St. Helens, 2004–2006* (chap. 26, U.S. Geological Survey Professional Paper 1750, pp. 543–571). https://doi.org/10.3133/pp1750

Giggenbach, W. F. (1975). A simple method for the collection and analysis of volcanic gas samples. *Bulletin Volcanologique*, *39*(1), 132–145. https://doi.org/10.1007/BF02596953

Giggenbach, W. F. (1996). Chemical composition of volcanic gases. In *Monitoring and mitigation of volcano hazards* (pp. 221–256). Retrieved from https://link.springer.com/chapter/10.1007/978-3-642-80087-0_7

Gillespie, A., Rokugawa, S., Matsunaga, T., Cothern, J. S., Hook, S., & Kahle, A. B. (1998). A temperature and emissivity separation algorithm for Advanced Spaceborne Thermal Emission and Reflection Radiometer (ASTER) images. *IEEE Transactions on Geoscience and Remote Sensing*, *36*(4), 1113–1126. https://doi.org/10.1109/36.700995

Global Volcanism Program. (2013). *Volcanoes of the World, v.4.9.0 (04 June 2020)*. Smithsonian Institution. https://doi.org/10.5479/si.GVP.VOTW4-2013

Goff, F., & Janik, C. J. (2002). Gas geochemistry of the Valles caldera region, New Mexico and comparisons with gases at Yellowstone, Long Valley and other geothermal systems. *Journal of Volcanology and Geothermal Research*, *116*, 299–323. https://doi.org/10.1016/S0377-0273(02)00222-6

Gong, W., Meyer, F. J., Lee, C. W., Lu, Z., & Freymueller, J. (2015). Measurement and interpretation of subtle deformation signals at Unimak Island from 2003 to 2010 using weather model- assisted time series InSAR. *Journal of Geophysical Research: Solid Earth*, *120*, 1175–1194. https://doi.org/10.1002/2014JB011384

Grapenthin, R., Freymueller, J. T., & Kaufman, A. M. (2013). Geodetic observations during the 2009 eruption of Redoubt Volcano, Alaska. *Journal of Volcanology and Geothermal Research*, *259*, 115–132. https://doi.org/10.1016/j.jvolgeores.2012.04.021

Greenland, L. P. (1987). Composition of gases from the 1984 eruption of Mauna Loa volcano. In R. W. Decker, T. L. Wright, & P. H. Stauffer (Eds.), *Volcanism in Hawaii* (chap. 30, U.S. Geological Survey Professional Paper 1350, pp. 781–790). https://doi.org/10.3133/pp1350

Harris, A. (2013). *Thermal remote sensing of active volcanoes: A user's manual* (p. 727). Cambridge University Press.

Hatch-Ibarra, R. L. (2020). *Characterization of recent earthquake sequences and swarms within the walker lane tectonic region* (Doctoral dissertation, p. 168). University of Nevada. Retrieved from https://scholarworks.unr.edu/handle/11714/7569

Henderson, S. T., Pritchard, M. E., Cooper, J. R., & Aoki, Y. (2019). Remotely sensed deformation and thermal anomalies at Mount Pagan, Mariana Islands. *Frontiers in Earth Science*, *7*, 238. https://doi.org/10.3389/feart.2019.00238

Hildreth, E. W., Fierstein, J., Lanphere, M. A., & Siems, D. F. (2001). Snowy Mountain: A pair of small andesite–dacite stratovolcanoes in Katmai National Park. In L. P. Gough & F. H. Wilson (Eds.), *Geologic studies in Alaska by the U.S. Geological survey, 1999* (U.S. Geological Survey Professional Paper 1633, pp. 13–34). https://doi.org/10.3133/pp1633

Hill, D. P. (1984). Monitoring unrest in a large silicic caldera, the Long Valley-Inyo craters volcanic complex in east-central California. *Bulletin Volcanologique*, *47*(2), 371–395.

Hill, D. P., & Prejean, S. (2005). Magmatic unrest beneath Mammoth Mountain, California. *Journal of Volcanology and Geothermal Research*, *146*(4), 257–283. https://doi.org/10.1016/j.jvolgeores.2005.03.002

Hooper, A., Wright, T., Spaans, K., Walters, R., Elliott, J., Weiss, J., et al. (2018). *Towards global monitoring of tectonic and volcanic hazards using Sentinel-1*. In 20th EGU General Assembly, EGU2018, Proceedings from the Conference (Vol. 20, p. 10855). Retrieved from http://adsabs.harvard.edu/abs/2018EGUGA.2010855H[Doi_inserted_from_Crossref

Howle, J. F., Langbein, J. O., Farrar, C. D., & Wilkinson, S. K. (2003). Deformation near the Casa Diablo geothermal well field and related processes Long Valley caldera, Eastern California, 1993–2000. *Journal of Volcanology and Geothermal Research*, *127*(3–4), 365–390. https://doi.org/10.1016/S0377-0273(03)00177-X

Ingebritsen, S. E., & Mariner, R. H. (2010). Hydrothermal heat discharge in the Cascade Range, northwestern United States. *Journal of Volcanology and Geothermal Research*, *196*(3-4), 208–218. https://doi.org/10.1016/j.jvolgeores.2010.07.023

Intrieri, E., Di Traglia, F., Del Ventisette, C., Gigli, G., Mugnai, F., Luzi, G., & Casagli, N. (2013). Flank instability of Stromboli volcano (Aeolian Islands, Southern Italy): Integration of GB-InSAR and geomorphological observations. *Geomorphology*, *201*, 60–69. https://doi.org/10.1016/j.geomorph.2013.06.007

Jiang, J., & Lohman, R. B. (2020). Coherence-guided InSAR deformation analysis in the presence of ongoing land surface changes in the Imperial Valley, California. *Remote Sensing of Environment*, *253*, 112160. https://doi.org/10.1016/j.rse.2020.112160

Kearney, C. (2005). *Detection of volcanic SO_2 in the North Pacific region using ASTER and MODIS* (Doctoral dissertation). University of Alaska Fairbanks.

Kienholz, C., Prakash, A., & Kolker, A. (2009). *Geothermal exploration in Akutan, Alaska, using multitemporal thermal infrared images*. American Geophysical Union Fall Meeting, Abstract H53F-1009.

Kilgore, W. W., Roman, D. C., Biggs, J., & Hansen, R. (2011). Seismic and geodetic investigation of the 1996–1998 earthquake swarm at Strandline Lake, Alaska. *Geophysical Journal International*, *186*(3), 1365–1379. https://doi.org/10.1111/j.1365-246X.2011.05115.x

Koyanagi, R., Kojima, G., Chong, F., & Chong, R. (1993). *Seismic monitoring of earthquakes and volcanoes in the Northern Mariana Islands: 1993 summary report*. Prepared for the Office of the Governor, Commonwealth of the Northern Mariana Islands (p. 34).

Kwoun, O. I., Lu, Z., Neal, C., & Wicks, C., Jr. (2006). Quiescent deformation of the Aniakchak Caldera, Alaska, mapped by InSAR. *Geology*, *34*(1), 5–8. https://doi.org/10.1130/G22015.1

Lanza, F., Roman, D. C., Power, J. A., & Thurber, C. H. (2020). *Insights into the 2020 earthquake swarm at Makushin volcano, Alaska from relative relocations and focal mechanisms*. American Geophysical Union Fall Meeting, Abstract (V020-0006).

Lerner, A. H., O'Hara, D., Karlstrom, L., Ebmeier, S. K., Anderson, K. R., & Hurwitz, S. (2020). The prevalence and significance of offset magma reservoirs at arc volcanoes. *Geophysical Research Letters*, *47*, e2020GL087856. https://doi.org/10.1029/2020GL087856

Lockwood, J., Banks, N., English, T., Greenland, P., Jackson, D., Johnson, D., et al. (1985). The 1984 eruption of Mauna Loa Volcano, Hawaii. *Eos, Transactions American Geophysical Union*, *66*(16), 169–171.

Lopez, T. M., Carn, S., Werner, C., Fee, D., Kelly, P., Doukas, M., et al. (2013). Evaluation of Redoubt Volcano's sulfur dioxide emissions by the Ozone Monitoring Instrument. *Journal of Volcanology and Geothermal Research*, *259*, 290–307. https://doi.org/10.1016/j.jvolgeores.2012.03.002

Lopez, T. M., Clarisse, L., Schwaiger, H., Van Eaton, A., Loewen, M., Fee, D., et al. (2020). Constraints on eruption processes and event masses for the 2016–2017 eruption of Bogoslof volcano, Alaska, through evaluation of IASI satellite SO_2 masses and complementary datasets. *Bulletin of Volcanology*, *82*(2), 17. https://doi.org/10.1007/s00445-019-1348-z

Lopez, T. M., Fischer, T. P., Plank, T. A., Malinverno, A., Rizzo, A. L., Rasmussen, D. J., et al. (2019). *Along-arc variations in volatile cycling across the Aleutian Arc*. AGU Fall Meeting, Abstract V53C-05.

Lopez, T. M., Tassi, F., Aiuppa, A., Galle, B., Rizzo, A. L., Fiebig, J., et al. (2017). Geochemical constraints on volatile sources and subsurface conditions at Mount Martin, Mount Mageik, and Trident Volcanoes, Katmai Volcanic Cluster, Alaska. *Journal of Volcanology and Geothermal Research*, *347*, 64–81. https://doi.org/10.1016/j.jvolgeores.2017.09.001

Lu, Z. (2007). InSAR imaging of volcanic deformation over cloud-prone areas—Aleutian Islands. *Photogrammetric Engineering & Remote Sensing*, *73*(3), 245–257. https://doi.org/10.14358/PERS.73.3.245

Lu, Z., & Dzurisin, D. (2014). *InSAR imaging of Aleutian Volcanoes. InSAR imaging of Aleutian Volcanoes* (pp. 87–345). Springer.

Lu, Z., Wicks, C., Jr., Power, J. A., & Dzurisin, D. (2000). Ground deformation associated with the March 1996 earthquake swarm at Akutan volcano, Alaska, revealed by satellite radar interferometry. *Journal of Geophysical Research*, *105*(B9), 21483–21495.

Lynch, D. K., Hudnut, K. W., & Adams, P. M. (2013). Development and growth of recently-exposed fumarole fields near Mullet Island, Imperial County, California. *Geomorphology*, *195*, 27–44. https://doi.org/10.1016/j.geomorph.2013.04.022

Lyons, J. J., Haney, M. M., Werner, C., Kelly, P., Patrick, M., Kern, C., & Trusdell, F. (2016). Long period seismicity and very long period infrasound driven by shallow magmatic degassing at Mount Pagan, Mariana Islands. *Journal of Geophysical Research: Solid Earth*, *121*, 188–209. https://doi.org/10.1002/2015JB012490

Marshall, G. A., Langbein, J., Stein, R. S., Lisowski, M., & Svarc, J. (1997). Inflation of Long Valley Caldera, California, Basin and Range strain, and possible Mono Craters dike opening from 1990–94 GPS surveys. *Geophysical Research Letters*, *24*(9), 1003–1006.

Mazzini, A., Svensen, H., Etiope, G., Onderdonk, N., & Banks, D. (2011). Fluid origin, gas fluxes and plumbing system in the sediment-hosted Salton Sea Geothermal System (California, USA). *Journal of Volcanology and Geothermal Research*, *205*, 67–83. https://doi.org/10.1016/j.jvolgeores.2011.05.008

McCormick, B., Popp, C., Andrews, B., & Cottrell, E. (2015). Ten years of satellite observations reveal highly variable sulphur dioxide emissions at Anatahan Volcano, Mariana Islands. *Journal of Geophysical Research: Atmospheres*, *120*, 7258–7282. https://doi.org/10.1002/2014JD022856

McGee, K. A., Doukas, M. P., McGimsey, R. G., Neal, C. A., & Wessels, R. L. (2010). Emission of SO_2, CO_2, and H_2S from Augustine Volcano, 2002–2008: Chapter 26 of Power,. In J. A. Power, M. L. Coombs, & J. T. Freymueller (Eds.), The 2006 eruption of Augustine Volcano, Alaska (U.S. Geological Survey Professional Paper 1769, pp. 609–627). https://doi.org/10.3133/pp176926

McGimsey, R. G., Neal, C. A., Girina, O. A., Chibisova, M. V., & Rybin, A. V. (2014). *2009 volcanic activity in Alaska, Kamchatka, and the Kurile Islands—Summary of events and response of the Alaska Volcano Observatory* (U.S. Geological Survey Scientific Investigations Report 2013-5213, p. 125). https://doi.org/10.3133/sir20135213

McLaughlin, R. J., & Donnelly-Nolan, J. M. (1981). *Research in the Geysers-Clear Lake geothermal area, northern California* (U.S. Geological Survey Professional Paper 1141). https://doi.org/10.3133/pp1141

Miller, T. P., McGimsey, R. G., Richter, D. H., Riehle, J. R., Nye, C. J., Yount, M. E., & Dumoulin, J. A. (1998). *Catalog of the historically active volcanoes of Alaska* (U.S. Geological Survey Open-File Report 98-582, p. 104). https://doi.org/10.3133/ofr98582

Mitchell, E. C., Fischer, T. P., Hilton, D. R., Hauri, E. H., Shaw, A. M., de Moor, J. M., et al. (2010). Nitrogen sources and recycling at subduction zones: Insights from the Izu-Bonin-Mariana arc. *Geochemistry, Geophysics, Geosystems*, *11*, Q02X11. https://doi.org/10.1029/2009GC002783

Moran, S., Freymueller, J., LaHusen, R. G., McGee, K. A., Poland, M. P., Power, J. A., et al. (2008). *Instrumentation recommendations for volcano monitoring at US volcanoes under the National Volcano Early Warning System* (U.S. Geological Survey Scientific Investigations Report 2008-5114). https://doi.org/10.3133/sir20085114

Motyka, S. A., Liss, S. A., Nye, C. J., & Moorman, M. A. (1993). *Geothermal resources of the Aleutian arc. Department of Natural Resources, State of Alaska* (Division of Geological and Geophysical Surveys. Professional Report 114, p. 21). Retrieved from https://dggs.alaska.gov/webpubs/dggs/pr/text/pr114.pdf

Moussa, D. A., & Kiser, E. (2018). *Seismicity beneath the Indian heaven volcanic field, Washington State, USA*. American Geophysical Union Fall Meeting Abstracts (V33D-0252).

Moxham, R. M. (1970). Thermal features at volcanoes in the cascade range, as observed by aerial infrared surveys. *Bulletin Volcanologique*, *34*(1), 77–106. https://doi.org/10.1007/BF02597780

Murphy, R., Thurber, C., Prejean, S., & Bennington, N. (2014). Three-dimensional seismic velocity structure and earthquake relocations at Katmai, Alaska. *Journal of Volcanology and Geothermal Research*, *276*, 121–131. https://doi.org/10.1016/j.jvolgeores.2014.02.022

Nathenson, M., & Mariner, R. H. (2013). *Springs, streams, and gas vent on and near Mount Adams volcano, Washington* (U.S. Geological Survey Scientific Investigations Report 2013-5097, p. 19). https://doi.org/10.3133/sir20135097

National Academies of Sciences, Engineering, and Medicine. (2018). *Thriving on our changing planet: A decadal strategy for Earth observation from space*. The National Academies Press. https://doi.org/10.17226/24938

Neal, C. A., Brantley, S. R., Antolik, L., Babb, J. L., Burgess, M., Calles, K., et al. (2019). The 2018 rift eruption and summit collapse of Kīlauea Volcano. *Science*, *363*(6425), 367–374. https://doi.org/10.1126/science.aav7046

Neal, C. A., McGimsey, R. G., Dixon, J. P., Manevich, A., & Rybin, A. (2009). *2006 volcanic activity in Alaska, Kamchatka, and the Kurile Islands: Summary of events and response of the Alaska Volcano Observatory* (U.S. Geological Survey Scientific Investigations Report 2008-5214, p. 102). https://doi.org/10.3133/sir20085214

Newhall, C. G., Costa, F., Ratdomopurbo, A., Venezky, D. Y., Widiwijayanti, C., Zar Win, N. T., et al. (2017). WOVOdat—An online, growing library of worldwide volcanic unrest. *Journal of Volcanology and Geothermal Research*, *345*, 184–199. https://doi.org/10.1016/j.jvolgeores.2017.08.003

Niu, Y. F., Dzurisin, D., & Lu, Z. (2019). Interferometric synthetic aperture radar study of recent eruptive activity at Shrub mud volcano, Alaska. *Journal of Volcanology and Geothermal Research*, *387*, 106671. https://doi.org/10.1016/j.jvolgeores.2019.106671

Okubo, P. G., & Wolfe, C. J. (2008). Swarms of similar long-period earthquakes in the mantle beneath Mauna Loa Volcano. *Journal of Volcanology and Geothermal Research*, *178*(4), 787–794. https://doi.org/10.1016/j.jvolgeores.2008.09.007

Patrick, M. R., & Witzke, C. N. (2011). *Thermal mapping of Hawaiian volcanoes with ASTER satellite data* (U.S. Geological Survey Scientific Investigations Report 2011-5110, p. 22). https://doi.org/10.3133/sir20115110

Pesicek, J. D., Wellik, J. J., Prejean, S. G., & Ogburn, S. E. (2018). Prevalence of seismic rate anomalies preceding volcanic eruptions in Alaska. *Frontiers of Earth Science*, *6*, 100. https://doi.org/10.3389/feart.2018.00100

Phillipson, G., Sobradelo, R., & Gottsmann, J. (2013). Global volcanic unrest in the 21st century: An analysis of the first decade. *Journal of Volcanology and Geothermal Research*, *264*, 183–196. https://doi.org/10.1016/j.jvolgeores.2013.08.004

Pieri, D. C., Abrams, M. J., & Tan, H. L. (2007). *Eruptions on a virtual globe: The Aster Volcano Archive*. American Geophysical Union, Fall Meeting 2007, Abstract Id. IN33A-0868. Retrieved from http://adsabs.harvard.edu/abs/2007AGUFMIN33A0868P

Poland, M. P. (2010). Localized surface disruptions observed by InSAR during strong earthquakes in Java and Hawaiʻi. *Bulletin of the Seismological Society of America*, *100*(2), 532–540. https://doi.org/10.1785/0120090175

Poland, M. P., Lisowski, M., Dzurisin, D., Kramer, R., McLay, M., & Pauk, B. (2017). Volcano geodesy in the Cascade arc, USA. *Bulletin of Volcanology*, *79*(8), 59. https://doi.org/10.1007/s00445-017-1140-x

Poland, M. P., Lopez, T., Wright, R., & Pavolonis, M. J. (2020). Forecasting, detecting, and tracking volcanic eruptions from space. *Remote Sensing in Earth Systems Sciences*, *3*(1), 55–94. https://doi.org/10.1007/s41976-020-00034-x

Poland, M. P., Miklius, A., & Montgomery-Brown, E. K. (2015). Magma supply, storage, and transport at shield-stage Hawaiian Volcanoes. In *Characteristics of Hawaiian volcanoes* (pp. 179–234).

Poland, M. P., Reath, K., Pritchard, M. E., Andrews, B. J., Bagnardi, M., Biggs, J., et al. (2019). *Multi-parameter volcano monitoring from space: Recommendations from the USGS Powell Center Volcano Remote Sensing Working Group and Beyond (abstract)*. Paper presented at 2019 SAGE/GAGE Workshop: Earth in 4D: Bridging the Timescales in Dynamic Earth Processes.

Potter, S. H., Scott, B. J., Jolly, G. E., Neall, V. E., & Johnston, D. M. (2015). Introducing the Volcanic Unrest Index (VUI): A tool to quantify and communicate the intensity of volcanic unrest. *Bulletin of Volcanology*, *77*(9), 77. https://doi.org/10.1007/s00445-015-0957-4

Power, J. A., Friberg, P. A., Haney, M. M., Parker, T., Stihler, S. D., & Dixon, J. P. (2019). *A unified catalog of earthquake hypocenters and magnitudes at volcanoes in Alaska—1989 to 2018* (U.S. Geological Survey Scientific Investigations Report 2019-5037, p. 17). https://doi.org/10.3133/sir20195037

Power, J. A., Roman, D. C., Lyons, J. J., & Haney, M. M. (2017). *Seismic observations of mount Cleveland, Alaska, a frequently active volcano in the Central Aleutian Arc*. Presented at the IAVCEI General Assembly.

Power, J. A., Stihler, S. D., Chouet, B. A., Haney, M. M., & Ketner, D. M. (2013). Seismic observations of Redoubt Volcano, Alaska—1989–2010 and a conceptual model of the Redoubt magmatic system. *Journal of Volcanology and Geothermal Research*, *259*, 31–44. https://doi.org/10.1016/j.jvolgeores.2012.09.014

Power, J. A., Stihler, S. D., White, R. A., & Moran, S. C. (2004). Observations of deep long-period (DLP) seismic events beneath Aleutian arc volcanoes; 1989–2002. *Journal of Volcanology and Geothermal Research*, *138*(3–4), 243–266. https://doi.org/10.1016/j.jvolgeores.2004.07.005

Pozgay, S. H., White, R. A., Wiens, D. A., Shore, P. J., Sauter, A. W., & Kaipat, J. L. (2005). Seismicity and tilt associated with the 2003 Anatahan eruption sequence. *Journal of Volcanology and Geothermal Research*, *146*(1–3), 60–76. https://doi.org/10.1016/j.jvolgeores.2004.12.008

Prejean, S., Ellsworth, W., Zoback, M., & Waldhauser, F. (2002). Fault structure and kinematics of the Long Valley Caldera region, California, revealed by high-accuracy earthquake hypocenters and focal mechanism stress inversions. *Journal of Geophysical Research*, *107*(B12), 2355. https://doi.org/10.1029/2001JB001168

Pritchard, M. E., Biggs, J., Wauthier, C., Sansosti, E., Arnold, D. W., Delgado, F., et al. (2018). Toward coordinated regional multi-satellite InSAR volcano observations: Results from the Latin America pilot project. *Journal of Applied Volcanology*, *7*(1), 1–28. https://doi.org/10.1186/s13617-018-0074-0

Pritchard, M. E., Mather, T. A., McNutt, S. R., Delgado, F. J., & Reath, K. (2019). Thoughts on the criteria to determine the origin of volcanic unrest as magmatic or non-magmatic. *Philosophical Transactions of the Royal Society A*, *377*(2139), 20180008. https://doi.org/10.1098/rsta.2018.0008

Reath, K. A., Pritchard, M., Moruzzi, S., Alcott, A., Coppola, D., & Pieri, D. (2019). The AVTOD (ASTER Volcanic Thermal Output Compilation) Latin America Archive. *Journal of Volcanology and Geothermal Research*, *376*, 62–74. https://doi.org/10.1016/j.jvolgeores.2019.03.019

Reath, K. A., Pritchard, M., Poland, M., Delgado, F., Carn, S., Coppola, D., et al. (2019). Thermal, deformation, and degassing remote sensing time series (CE 2000–2017) at the 47 most active volcanoes in Latin America: Implications for volcanic systems. *Journal of Geophysical Research: Solid Earth*, *124*, 195–218. https://doi.org/10.1029/2018JB016199

Reath, K. A., Ramsey, M., & Tratt, D. M. (2010). *Application of high-resolution thermal infrared sensors for geothermal exploration at the Salton Sea, California*. American Geophysical Union Fall Meeting, V23D-03.

Roman, D. C., & Cashman, K. V. (2018). Top-down precursory volcanic seismicity: Implications for 'stealth' magma ascent and long-term eruption forecasting. *Frontiers of Earth Science*, *6*, 124. https://doi.org/10.3389/feart.2018.00124

Roman, D. C., & Power, J. A. (2011). Mechanism of the 1996–97 non-eruptive volcano-tectonic earthquake swarm at Iliamna Volcano, Alaska. *Bulletin of Volcanology*, *73*(2), 143–153. https://doi.org/10.1007/s00445-010-0439-7

Sako, M. K., Trusdell, F. A., Koyanagi, R. Y., Kojima, G., & Moore, R. B. (1995). *Volcanic investigations in the commonwealth of the Northern Mariana Islands, April to May 1994* (U.S. Geological Survey Open-File Report 94-705, p. 57). https://doi.org/10.3133/ofr94705

Salzer, J. T., Nikkhoo, M., Walter, T. R., Sudhaus, H., Reyes-Dávila, G., Bretón, M., & Arámbula, R. (2014). Satellite radar data reveal short-term pre-explosive displacements and a complex conduit system at Volcán de Colima, Mexico. *Frontiers of Earth Science*, *2*, 12. https://doi.org/10.3389/feart.2014.00012

Schaefer, J. R., Scott, W. E., Evans, W. C., Jorgenson, J., McGimsey, R. G., & Wang, B. (2008). The 2005 catastrophic acid crater lake drainage, lahar, and acidic aerosol formation at Mount Chiginagak volcano, Alaska, USA: Field observations and preliminary water and vegetation chemistry results. *Geochemistry, Geophysics, Geosystems*, *9*, Q07018. https://doi.org/10.1029/2007GC001900

Schneider, D. J., & Rose, W. I. (1995). Tracking of the 1992 Crater Peak/Spurr eruption clouds using AVHRR. In T. E. C. Keith (Ed.), *The 1992 eruptions of Crater Peak Vent, Mount Spurr Volcano, Alaska* (chap. 3, U.S. Geological Survey Bulletin 2139, pp. 27–36). https://doi.org/10.3133/b2139

Sherrod, D. R., Mastin, L. G., Scott, W. E., & Schilling, S. P. (1997). *Volcano hazards at Newberry Volcano, Oregon* (United States Geological Survey Open-File Report 99-311).

Smith, K. D., Kent, G. M., von Seggern, D. P., Driscoll, N. W., & Eisses, A. (2016). Evidence for Moho-lower crustal transition depth diking and rifting of the Sierra Nevada microplate. *Geophysical Research Letters*, *43*, 10–738. https://doi.org/10.1002/2016GL070283

Smith, K. D., Von Seggern, D., Blewitt, G., Preston, L., Anderson, J. G., Wernicke, B. P., & Davis, J. L. (2004). Evidence for deep magma injection beneath Lake Tahoe, Nevada-California. *Science*, *305*(5688), 1277–1280. https://doi.org/10.1126/science.1101304

Symonds, R. B., Janik, C. J., Evans, W. C., Ritchie, B. E., Counce, D., Poreda, R. J., & Iven, M. (2003). *Scrubbing masks magmatic degassing during repose at Cascade-Range and Aleutian-Arc volcanoes* (U.S. Geological Survey Open-File Report 03-435). https://doi.org/10.3133/ofr03435

Symonds, R. B., Poreda, R. J., Evans, W. C., Janik, C. J., & Ritchie, B. E. (2003). *Mantle and crustal sources of carbon, nitrogen, and noble gases in Cascade-Range and Aleutian-Arc volcanic gases* (U.S. Geological Survey Open-File Report 03-436). https://doi.org/10.3133/ofr03436

Symonds, R. B., Reed, M. H., & Rose, W. I. (1992). Origin, speciation, and fluxes of trace-element gases at Augustine volcano, Alaska: Insights into magma degassing and fumarolic processes. *Geochimica et Cosmochimica Acta*, *56*(2), 633–657.

Syracuse, E. M., Maceira, M., Zhang, H., & Thurber, C. H. (2015). Seismicity and structure of Akutan and Makushin Volcanoes, Alaska, using joint body and surface wave tomography. *Journal of Geophysical Research: Solid Earth*, *120*, 1036–1052. https://doi.org/10.1002/2014JB011616

Thelen, W. A. (2016). *Seismicity of cascade volcanoes: Characterization and comparison*. American Geophysical Union Fall Meeting Abstracts V53C-3106.

Tizzani, P., Berardino, P., Casu, F., Euillades, P., Manzo, M., Ricciardi, G. P., et al. (2007). Surface deformation of Long Valley caldera and Mono Basin, California, investigated with the SBAS-InSAR approach. *Remote Sensing of Environment*, *108*(3), 277–289. https://doi.org/10.1016/j.rse.2006.11.015

Trugman, D. T., Shearer, P. M., Borsa, A. A., & Fialko, Y. (2016). A comparison of long-term changes in seismicity at The Geysers, Salton Sea, and Coso geothermal fields. *Journal of Geophysical Research: Solid Earth*, *121*, 225–247. https://doi.org/10.1002/2015JB012510

Trusdell, F. A., Moore, R. B., Sako, M., White, R. A., Koyanagi, S. K., Chong, R., & Camacho, J. T. (2005). The 2003 eruption of Anatahan Volcano, Commonwealth of the Northern Mariana Islands: Chronology, volcanology, and deformation. *Journal of Volcanology and Geothermal Research*, *146*(1–3), 184–207. https://doi.org/10.1016/j.jvolgeores.2004.12.010

UNESCO. (1971). *The surveillance and prediction of volcanic activity. A review of methods and techniques* (p. 200). UNESCO.

Vaughan, R. G., Keszthelyi, L. P., Lowenstern, J. B., Jaworowski, C., & Heasler, H. (2012). Use of ASTER and MODIS thermal infrared data to quantify heat flow and hydrothermal change at Yellowstone National Park. *Journal of Volcanology and Geothermal Research*, *233*, 72–89. https://doi.org/10.1016/j.jvolgeores.2012.04.022

Wagner, S. M., Varecamp, J. C., Cooke, C. A., Smith, C., Thomas, E., Cauley, C., & Tartell, P. (2018). *Volcanic mercury and CO_2 venting through East lake, Newberry Volcano, OR*. American Geophysical Union, Fall Meeting 2018, abstract #V43I-0252.

Wang, T., Poland, M. P., & Lu, Z. (2015). Dome growth at Mount Cleveland, Aleutian Arc, quantified by time series TerraSAR-X imagery. *Geophysical Research Letters*, *42*, 10–614. https://doi.org/10.1002/2015GL066784

Waythomas, C. F., Angeli, K., & Wessels, R. L. (2020). Evolution of the submarine–subaerial edifice of Bogoslof volcano, Alaska, during its 2016–2017 eruption based on analysis of satellite imagery. *Bulletin of Volcanology*, *82*(2), 1–26. https://doi.org/10.1007/s00445-020-1363-0

Waythomas, C. F., Scott, W. E., Prejean, S. G., Schneider, D. J., Izbekov, P., & Nye, C. J. (2010). The 7–8 August 2008 eruption of Kasatochi Volcano, central Aleutian Islands, Alaska. *Journal of Geophysical Research*, *115*, B00B06. https://doi.org/10.1029/2010JB007437

Wech, A. G., Tepp, G., Lyons, J., & Haney, M. (2018). Using earthquakes, T waves, and infrasound to investigate the eruption of Bogoslof volcano, Alaska. *Geophysical Research Letters*, *45*, 6918–6925. https://doi.org/10.1029/2018GL078457

Wech, A. G., Thelen, W. A., & Thomas, A. M. (2020). Deep long-period earthquakes generated by second boiling beneath Mauna Kea volcano. *Science*, *368*(6492), 775–779. https://doi.org/10.1126/science.aba4798

Werner, C. A., Doukas, M. P., & Kelly, P. J. (2011). Gas emissions from failed and actual eruptions from Cook Inlet Volcanoes, Alaska, 1989–2006. *Bulletin of Volcanology*, *73*(2), 155–173. https://doi.org/10.1007/s00445-011-0453-4

Werner, C. A., Evans, W. C., Poland, M., Tucker, D. S., & Doukas, M. P. (2009). Long-term changes in quiescent degassing at Mount Baker Volcano, Washington, USA; Evidence for a stalled intrusion in 1975 and connection to a deep magma source. *Journal of Volcanology and Geothermal Research*, *186*(3–4), 379–386. https://doi.org/10.1016/j.jvolgeores.2009.07.006

Werner, C. A., Hurwitz, S., Evans, W. C., Lowenstern, J. B., Bergfeld, D., Heasler, H., et al. (2008). Volatile emissions and gas geochemistry of Hot Spring Basin, Yellowstone National Park, USA. *Journal of Volcanology and Geothermal Research*, *178*(4), 751–762. https://doi.org/10.1016/j.jvolgeores.2008.09.016

Werner, C. A., Kelly, P. J., Doukas, M., Lopez, T., Pfeffer, M., McGimsey, R., & Neal, C. (2013). Degassing of CO_2, SO_2, and H_2S associated with the 2009 eruption of Redoubt Volcano, Alaska. *Journal of Volcanology and Geothermal Research*, *259*, 270–284. https://doi.org/10.1016/j.jvolgeores.2012.04.012

Werner, C. A., Kern, C., Coppola, D., Lyons, J. J., Kelly, P. J., Wallace, K. L., et al. (2017). Magmatic degassing, lava dome extrusion, and explosions from Mount Cleveland volcano, Alaska, 2011–2015: Insight into the continuous nature of volcanic activity over multi-year timescales. *Journal of Volcanology and Geothermal Research*, *337*, 98–110. https://doi.org/10.1016/j.jvolgeores.2017.03.001

Werner, C. A., Kern, C., & Kelly, P. K. (2020). *Chemical evaluation of water and gases collected from hydrothermal systems located in the central Aleutian arc, August 2015* (U.S. Geological Survey Scientific Investigations Report 2020-5043, p. 35). https://doi.org/10.3133/sir20205043

Werner, C. A., Rasmussen, D. J., Plank, T., Kelly, P. J., Kern, C., Lopez, T., et al. (2020). Linking subsurface to surface using gas emission and melt inclusion data at Mount Cleveland volcano, Alaska. *Geochemistry, Geophysics, Geosystems*, *21*, e2019GC008882. https://doi.org/10.1029/2019GC008882

West, M., Sanchez, J., & McNutt, S. (2005). Periodically triggered seismicity at Mount Wrangell, Alaska, after the Sumatra earthquake. *Science*, *308*, 1144–1146. https://doi.org/10.1126/science.1112462

Wicks, C. W., Thatcher, W., Monastero, F. C., & Hasting, M. A. (2001). Steady state deformation of the Coso Range, east central California, inferred from satellite radar interferometry. *Journal of Geophysical Research*, *106*(B7), 13769–13780. https://doi.org/10.1029/2001JB000298

Wittmann, W., Sigmundsson, F., Dumont, S., & Lavallée, Y. (2017). Post-emplacement cooling and contraction of lava flows: InSAR observations and a thermal model for lava fields at Hekla volcano, Iceland. *Journal of Geophysical Research: Solid Earth*, *122*, 946–965. https://doi.org/10.1002/2016JB013444

Wright, R. (2016). MODVOLC: 14 years of autonomous observations of effusive volcanism from space. *Geological Society, London, Special Publications*, *426*(1), 23–53. https://doi.org/10.1144/SP426.12

Wright, R., Flynn, L. P., Garbeil, H., Harris, A. J. L., & Pilger, E. (2004). MODVOLC: Near-real-time thermal monitoring of global volcanism. *Journal of Volcanology and Geothermal Research*, *135*(1–2), 29–49. https://doi.org/10.1016/j.jvolgeores.2003.12.008